UNIVERSITEIT VAN PRETORIA
UNIVERSITY OF PRETORIA
YUNIBESITHI YA PRETORIA

LEACHING OF CRUDE TITANIUM POWDER PRODUCED BY METALLOTHERMIC REDUCTION: EFFECTS OF LEACHING CONDITIONS ON FINAL POWDER QUALITY

BY

Matsie Rinny Serwale

Supervised by

Prof K.C. Sole, Dr T. Coetsee and Dr S. Fazluddin

A dissertation submitted in partial fulfilment of the requirements for the degree of

Master of Applied Sciences (Metallurgy)

in the

Department of Materials Science and Metallurgical Engineering

Faculty of Engineering, Built Environment and Information Technology

University of Pretoria

Republic of South Africa

2021

ABSTRACT

A low-cost titanium production process, the CSIR-Ti powder process, which aims to produce titanium powder directly by metallothermic reduction of titanium tetrachloride with lithium, has been under development at the Council for Industrial and Scientific Research (CSIR). Crude titanium powder produced using the CSIR-Ti process is inevitably contaminated with by-products such as lithium chloride, lithium and titanium dichloride. These by-products tend to become sources of impurities in titanium powder, specifically oxygen and chloride impurities. The presence of oxygen and chloride impurities has marked effects on the mechanical properties of titanium finished products. Consequently, for the crude titanium powder to be rendered useful downstream, it must be purified and the by-products reduced to concentrations specified in the commercial standards. The present study was undertaken to examine whether acid leaching could be used to selectively dissolve and prevent hydrolysis of the by-products—specifically excess lithium and unreacted titanium dichloride in the crude titanium powder produced by the CSIR-Ti process. A further objective was to determine whether a purified product that meets both oxygen and total residual chloride content as specified by the standards can be achieved. The effects of key leaching variables and their interaction were also investigated to gain fundamental understanding of these effects on the by-products leaching behaviour.

A literature study to select a suitable lixiviant and to establish the aqueous chemistry of the by-products and their effect on the leaching conditions was undertaken. It showed that of the various acids suggested in the literature, hydrochloric acid was the cheapest and that it was more suited for the CSIR-Ti leaching process than nitric acid, due to the common ion chloride. This simplifies the leachate purification process downstream. The literature study established that Ti(II) has no aqueous chemistry but instead is oxidised to Ti(III) in solution. It was found that Ti(III) is easily oxidised to TiO^{2+} by dissolved oxygen and water. However, the oxidation rate was slow in hydrochloric acid solutions with the advantage that hydrolysis of the ions could be minimised and the precipitation of the oxides or oxychlorides prevented. It was further revealed that the lithium neutralisation reaction is highly exothermic, with the possibility of raising the leachate temperature to 60°C, resulting in the contamination of the titanium powder particles by the oxide layer and precipitated hydrolysis products.

Batch leaching tests were carried out using factorial design of experiments to investigate the effect of initial hydrochloric acid concentration, which was estimated by varying the concentration

between 0.032 M and 1 M; particle size, which was varied between −10 mm and +10 mm; and the initial temperature, varied between 14°C and 30°C. The resulting data were modelled and analysed using the analysis of variance statistical method. The solid residues were analysed for oxygen and total residual chloride content. The solid residue was also characterised by scanning electron microscopy (SEM) to examine the morphology of the leached particles. Leaching kinetics model fitting was also conducted.

The statistical analysis showed that of the three factors investigated, temperature was the factor with the most statistical significance on both the oxygen and chloride concentration in the purified product, followed by particle size. The effect of acid concentration proved to be minimal, a phenomenon attributed to low concentrations of acid-consuming impurities, specifically excess lithium in the crude product. Thus, the two concentrations of hydrochloric acid investigated were found to be efficient to prevent hydrolysis product formation.

Scanning electron micrographs revealed that crushing the crude product with a jaw crusher occluded crude titanium pores, thus locking in some by-products in addition to the pores locked by sintering during the metallothermic reduction. The observation showed that residual chloride impurities in the purified product are not just a consequence of hydrolysis products but also by-products locked deeper in the pores of the product.

Based on the parameter ranges evaluated in the study, a product that satisfied both oxygen and chloride standard specifications was achieved when the crude product was leached in both 1 M and 0.032 M initial HCl concentrations, temperature of 30°C and particle size of +10 mm. The combination of (−10 mm and 14°C) at all concentrations also yielded acceptable oxygen and chloride content levels. Overall, it was concluded from the present work that purification of crude CSIR-Ti product by leaching in dilute HCl is technically feasible.

Keywords: titanium powder, titanium sponge, acid leaching, oxygen, chlorine, by-products, CSIR-Ti process

ACKNOWLEDGEMENTS

I would like to extend my sincerest gratitude to my supervisors Prof K C Sole, Dr T Coetsee and Dr S Fazluddin, for their esteemed supervision, interest and constructive criticism in this work.

The author also wishes to express her appreciation to the following:

The staff members at the Titanium Centre of Competence (TiCoC) pilot plant, particularly the primary processing metals group (Mr J Skhosana and Mr J Swanepoel), for their cooperation, unending assistance and the provision of samples.

Mrs Belinda-Leigh Hickman (NECSA) for the chloride analysis.

Dr K Mutombo, Mr I Monareng and Mr B Sehoana for their assistance with the SEM analysis.

Mr Alan Scrooby (Scroobys Laboratory Service CC) for all the assistance regarding the head sample oxygen content assays.

The Council for Scientific and Industrial Research (CSIR) and the Department of Science and Technology (DST) for financial support.

Finally, a special thank you to my family for their unconditional love and emotional support throughout my studies.

DECLARATION

1. I understand what plagiarism is and am aware of the University's policy in this regard.
2. I declare that this dissertation is my own original work. Where other people's work has been used (either from a printed source, Internet or any other source), this has been properly acknowledged and referenced in accordance with departmental requirements.
3. I have not used work previously produced by another student or any other person to hand in as my own.
4. I have not allowed and will not allow anyone to copy my work with the intention of passing it off as his or her own work.

Signature: 

Date: 05/05/2021

TABLE OF CONTENTS

LIST OF TABLES

LIST OF FIGURES

1 INTRODUCTION

1.1 Motivation and background

Titanium (Ti) is an allotropic element revered for its renowned properties, including its high specific strength-to-mass ratio, biocompatibility and excellent corrosion resistance (Chown, 2016; Fang et al., 2018). Combinations of these properties render titanium and its alloys suitable for various applications in a broad spectrum of industries ranging from chemicals, medical to aerospace (Wang et al., 2013). Despite the fact that titanium has remarkable properties, it has still not reached the common metal status due to the high cost associated with its production and fabrication (Oosthuizen & Swanepoel, 2018). This pertinent issue has driven the industry to explore alternative process routes to conventional ingot metallurgy (Peter et al., 2012).

Powder metallurgy (PM) was identified as an alternative method that can reduce total component manufacturing costs. The use of PM enables the use of near net shape techniques, thus eliminating the wastage associated with conventional wrought metallurgical processes (Hansen & Gerdemann, 1998). Furthermore, the fine grain size used in PM enhances mechanical properties, making it possible to manufacture alloys that may not be possible with ingot metallurgy (Hansen & Gerdemann, 1998). However, Ti-PM is also limited to niche applications because all commercial methods to produce titanium powder make use of titanium sponge as a precursor, which adds cost to existing commercial technologies (Van Vuuren et al., 2011). Researchers have argued that the high cost of titanium powder is the hurdle limiting Ti-PM technology (Fang et al., 2018; Peter et al., 2012).

A low-cost titanium manufacturing process, the CSIR-Ti powder process, which aims to produce titanium particulate as the product of the metallothermic reduction of titanium tetrachloride ($TiCl_4$) with lithium (Li), has been under development at the South African Council for Industrial and Scientific Research (CSIR). The metallothermic reduction is believed to occur stepwise, with the intermediate formation of titanium trichloride ($TiCl_3$) and titanium dichloride ($TiCl_2$) (Liang et al., 2018). The process yields a crude product encapsulated in lithium chloride (LiCl) and, depending on whether the metallothermic reduction is completed with either stoichiometric excess Li or $TiCl_4$, may also have traces of excess Li, $TiCl_3$ and $TiCl_2$.

The challenge with titanium powder derived directly from metallothermic reduction processes without being subsequently melted, is the presence of impurities from residual reaction by-products. This challenge is also experienced in the commercially established hydride de-hydride (HDH) powder production process (Baril et al., 2011; Yan et al., 2015). Residual by-products are detrimental to titanium mechanical characteristics (Peter et al., 2012); for instance, chlorine has volatile behaviour at high temperature, resulting in macroporosity, which degrades fatigue properties (Yan et al., 2015). Oxygen changes phase selection and microstructure, which increases elastic modulus and yield strength in titanium, thus reducing ductility (Baril et al., 2011). The challenge encountered in all alternative methods to produce titanium powder economically is the removal of by-products in the crude product (Liang et al., 2020; Peter et al., 2012).

The separation of by-products to achieve a product adhering to specifications is achieved by either vacuum distillation or leaching. The decision to select a suitable purification method depends mainly on the solubility and volatility of the by-products to be separated, operating cost, downstream requirements for recycling the halide salt and quality of the final product (Van Vuuren, 2009).

Vacuum distillation has the advantage that both purification and metallothermic reduction can be accomplished in a single station (Nagesh et al., 1994). This results in a superior quality product with the lowest oxygen content of all purification methods (Nagesh et al., 2008). Despite the efforts to optimise vacuum distillation, the process remains a crucial cost component during titanium sponge production because of the prolonged heating times required due to inefficient heat transfer (Liang et al., 2018). The high operating temperature of 950°C to 1000°C used in the vacuum distillation process tends to sinter and alter the product morphology (Gambogi & Gerdemann, 1999; Hansen & Gerdemann, 1998; Liang et al., 2018).

Leaching has the advantage that it is not energy-intensive and large quantities of salt can be removed at a relatively low cost due to the simple equipment required (McKinley, 1955). Drawbacks with this method include the low concentration of recycled by-products due to water dilution and contamination of the product by the leaching liquor (Hansen & Gerdemann, 1998). However, leaching is used successfully in the Hunter process (Gambogi & Gerdemann, 1999).

The salt by-product in the crude reaction mass produced by the CSIR-Ti process is not drained and, given that it is postulated that the crude product contains almost 78% salt by-product in contrast to the 15%–20% salt by-product in the Kroll process, additional time and energy will be

required to vacuum distil all the salt (Aleksandrovskii et al., 1982; Gambogi & Gerdemann, 1999; Garmata et al., 1970).

Based on the solubility and the technical points stated, it was decided that, in the effort to lower production cost, leaching might be a suitable purification method for the CSIR-Ti crude product. However, the method is complicated by a series of side reactions between the by-products and water, which result in the formation of insoluble hydrolysis products. The hydrolysis products precipitate out and concentrate on the metal surface and in the metal pores, thus contaminating it with oxides and oxychlorides (Garmata et al., 1970; Jamrack, 1963). In addition to the problem stated above, is the development of heat resulting from the dissolution of the by-products in water. The exothermic heat of dissolution favours rapid precipitation of hydrolysis products, as well as oxidation of titanium, as pointed out by Garmata et al. (1970), who indicated that when the crude product was leached at temperatures between 30˚C to 40˚C, the titanium oxygen content was 0.025% and increased to between 0.10% at 100˚C, 0.15% at 150˚C and 0.2% at 200˚C.

It has been established that hydrolysis reactions can be minimised or inhibited in aqueous acidified solution because the precipitation of hydrolysis products is slow under these conditions (Jamrack, 1963; Kelly, 1963). Consequently, it is possible to recover lower valence chlorides in the leachate as ions in solution, thus counteracting the disadvantages associated with leaching. The exothermic heat of reaction can be circumvented by controlling the feed rate, agitation speed and installing an external cooling jacket (Garmata et al., 1970).

1.2 Research aim and objectives

The principal aim of this study was to investigate the feasibility of utilising acid leaching to purify crude-Ti product derived by metallothermic reduction to achieve commercially pure (CP) grade specifications for oxygen and chlorine. These objectives were achieved by:

1. Completing a literature survey to evaluate open literature regarding titanium and lithium aqueous chemistry to identify and select a suitable lixiviant, inclusive of a concentration to prevent the formation of hydrolysis products.
2. Conducting leaching tests to investigate the effect of temperature, particle size and acid concentration on the final product quality.
3. Testing the applicability of mathematical models on the leaching kinetics.

1.3 Scope of this study

Of the various facets that make up quality in the titanium industry, the study was limited to purity, specifically, oxygen and chlorine, because these impurities are difficult to remove (Liang et al., 2018; Peter et al., 2012; Yan et al., 2015). For instance, oxygen is an interstitial impurity that dissolves in titanium and cannot be removed by employing vacuum melting processes (Xia et al., 2019; Yan et al., 2015). Chlorides are insoluble in titanium (Low et al., 2012). Mitigation efforts such as scavenging with yttrium oxide and increased vacuum distillation residence time have been relatively impractical and ineffective due to the additional costs associated with the procedures (Low et al., 2012). Other contaminants were beyond the scope of the research.

1.4 Dissertation layout

Chapter 1 of this dissertation introduces the background as well as the motivation for the research work. Chapter 2 reviews the available literature to establish bounds of knowledge on titanium purification methods, focusing on acid leaching and establishing the parameters that meet the specified quality requirements. Chapters 3 and 4 present the methodology, and results and discussion, respectively. Chapter 5 presents the conclusions of the dissertation as well as recommendations for future research.

2 LITERATURE REVIEW

2.1 General background

Titanium is extracted from oxygen-bearing minerals, primarily the following economically significant minerals: rutile, ilmenite and leucoxene (Gambogi & Gerdemann, 1999). Of the three minerals, ilmenite is the most abundant, and recent data from the U.S. Geological Survey (2020), indicate that it accounts for 89% of the global consumption. Extraction of titanium by conventional carbothermic reduction is impossible because at high temperature TiO_2 in the presence of carbon is transformed into a highly stable carbide (Clark, 1973). The tendency to form interstitial compounds at high temperatures is not limited to carbon but exists for other elements such as nitrogen and oxygen (Garmata et al., 1970). Consequently, all fabrication processes are performed under argon gas (Ar) because minute quantities of these elements exert considerable effects on the mechanical properties of titanium (Wasz et al., 1996).

2.2 Conventional methods for producing titanium metal

2.2.1 Feedstock preparation

The primary industrial process for producing commercially pure titanium metal is based on chloride metallurgy as the method has the advantage of producing high-purity titanium (Van Vuuren, 2009). This is accomplished by carrying out the reduction process in an oxygen-free system, with the production of $TiCl_4$, which is the established feedstock for all commercial processes (Gambogi & Gerdemann, 1999; Van Tonder, 2010). Titanium tetrachloride is synthesised by chlorination of natural or synthetic rutile obtained from $FeTiO_3$ or TiO_2-rich slag with chlorine and petroleum coke in a fluidised bed reactor at 1100–1200°C (Habashi, 1997; Kohli, 1981), as summarised by equation [2.1]:

$$TiO_2(s) + C(s) + 2\,Cl_2(g) \rightarrow TiCl_4(g) + CO_2(g) \qquad [2.1]$$

The product generated by chlorination is not pure and usually contains 94% $TiCl_4$ contaminated with trace metal chlorides such as aluminium chloride, ferric chloride and vanadium oxychloride from the precursors (Habashi, 1997; Kohli, 1981).

Crude $TiCl_4$ is purified further by a combination of processes, which include precipitation and fractional distillation to obtain $TiCl_4$ with purity above 99.98% (Habashi, 1997).

2.2.2 Conventional metal production methods

Commercially accepted methods to produce titanium metal ingots and powder involve producing an agglomerated mass referred to as titanium sponge. The sponge is produced by the metallothermic reduction of $TiCl_4$ with either molten magnesium (Mg) in a process termed the Kroll process or sodium (Na) in the alternative Hunter process (Nagesh et al., 2008). The processing steps for both processing routes are shown in Figure 2.1.

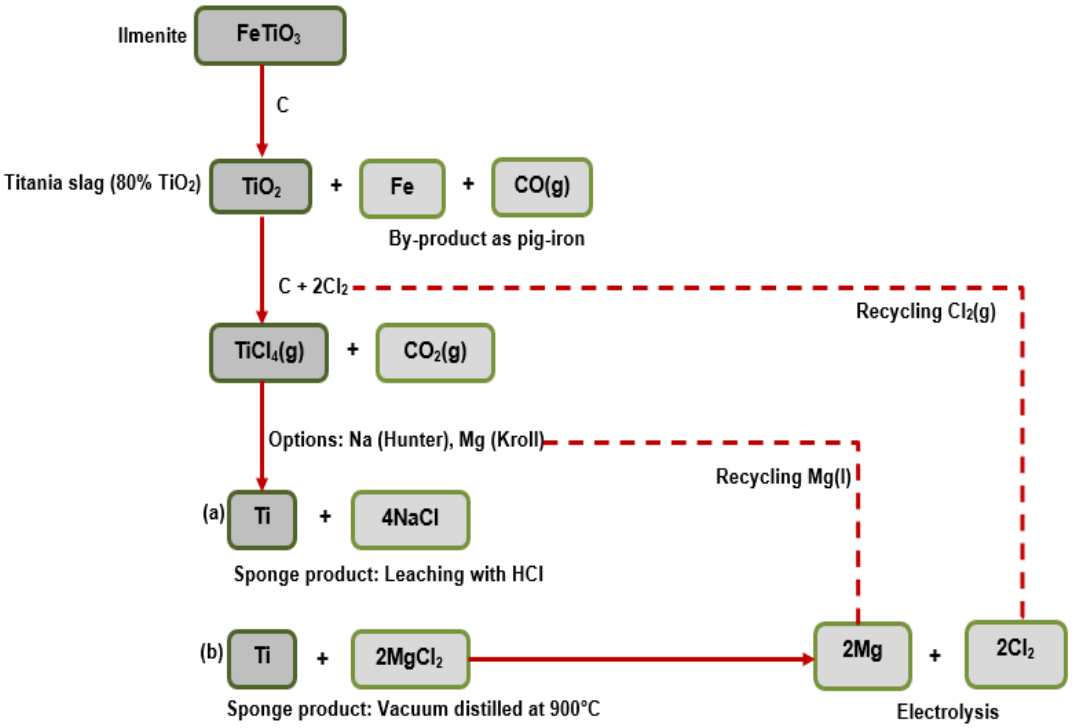

Figure 2.1 Chemical pathways, with reactions and respective products, of the two commercial processes used to produce titanium metal: (a) Hunter and (b) Kroll processes (Van Tonder, 2010).

The Kroll process is a batch-type process conducted in a sealed reactor under Ar atmosphere. In this process, a required quantity of metallic Mg plus an excess of 15%–30% is charged into a retort and heated to 850°C (Gambogi & Gerdemann, 1999), followed by controlled addition of $TiCl_4$ to control the exothermic heat of reaction to maintain the temperature at approximately 900°C, to ensure the smooth running of the process (Ivanov & Zablotsky, 2018). Owing to its low boiling point of 136°C, $TiCl_4$ vaporises and reacts with molten Mg to produce titanium sponge and magnesium chloride salt ($MgCl_2$) according to reaction [2.2].

$$TiCl_4(g) + 2\,Mg(l) \rightarrow Ti(s) + 2\,MgCl_2(l) \quad [2.2]$$

While the reaction defined in equation [2.2] appears to be a straightforward displacement reaction, experimental and theoretical evidence indicates that the metallothermic reduction of $TiCl_4$ is a complex stepwise heterogeneous reaction (Liang et al., 2019). The reaction proceeds via intermediate stages to form lower valence titanium chlorides commonly referred to as sub-chlorides, such as $TiCl_2$ and $TiCl_3$ (Liang et al., 2019; Nagesh et al., 2004). The reaction path is said to be unclear, but it is accepted that the direction in which the reaction can proceed is determined by thermodynamics, and the extent of the reactions by kinetics, which depend on the interaction of the different phases (gas, liquid, solid) (Ivanov & Zablotsky, 2018; Nagesh et al., 2004). All these reactions effectively reduce to equation [2.2]. The first most probable pathway comprises reducing vapourised $TiCl_4$ by molten Mg or vapours of Mg via equation [2.3], to form $TiCl_3$ and $MgCl_2$:

$$2\,TiCl_4(g) + Mg(l/g) \rightarrow 2\,TiCl_3(g) + MgCl_2(l) \quad [2.3]$$

Nagesh et al. (2004) deduced that after this initial reaction [2.3], further magnesiothermic reduction of $TiCl_4$ and $TiCl_3$ proceeds via two significant multicomponent reactions [2.4] and [2.5] to form $TiCl_3$ and $TiCl_2$. The reactions involve the dissolution of reagents in the molten salt by-product ($MgCl_2$) as well as the transportation of the salt or gas thereof:

$$2\,TiCl_4(g) + Mg\left(\text{in } MgCl_2\right) \rightarrow 2\,TiCl_3(g) + MgCl_2(l) \quad [2.4]$$

$$TiCl_4/_{TiCl_3}(g) + Mg(g) \rightarrow TiCl_2\left(\text{in } MgCl_2\right) + MgCl_2(l) \quad [2.5]$$

$$TiCl_2\left(\text{in } MgCl_2\right) + Mg \text{ in } \left(MgCl_2\right) \rightarrow Ti(s) + MgCl_2(l) \quad [2.6]$$

The final step in producing sponge is achieved by the reduction of dissolved $TiCl_2$ (in $MgCl_2$) by either Mg (in $MgCl_2$) according to equation [2.6], or by the electronically mediated reaction on any conductive surface, as discussed elsewhere in the literature (Ivanov & Zablotsky, 2018; Okabe & Waseda, 1997). During reduction, molten $MgCl_2$ settles below the molten Mg, but above the sponge, due to the differences in specific gravity, and is periodically tapped from the reactor to ensure effective reactor volume utilisation (Nagesh et al., 2008). Most literature suggests that of

the Mg reductant charged, about 30% does not react with $TiCl_4$ because it is occluded in the sponge pores and cannot reach the reaction interphase (Gambogi & Gerdemann, 1999; Garmata et al., 1970).

In the alternative Hunter process, the reaction steps are similar to the Kroll process as indicated in Figure 2.1(a). The critical difference between the two processes is that the reducing metal Mg is substituted with Na, as in equation [2.7]:

$$TiCl_4(g) + 4\ Na(l) \rightarrow Ti(s) + 4\ NaCl(l) \qquad [2.7]$$

The process is operated at a temperature of approximately 900°C, a temperature at which NaCl is in the molten state, to prevent cold pocket formation in the reduction retort. The NaCl salt by-product formed is not withdrawn but allowed to accumulate in the reactor due to the high solubility of Na in NaCl (Aleksandrovskii et al., 1982). A stoichiometric excess of 5%–15% $TiCl_4$ is introduced at the end of the reduction process to consume any unreacted Na to mitigate the safety hazards associated with the reactions between excess Na and air or water (Jamrack, 1963). Additional differences between the two processes emanate from the reaction mechanism, a consequence of the tendency of sodium to be volatile (b.p. 883°C) and to boil under reflux during the reaction, resulting in a reaction principally via the vapour phase. Thus, the sponge produced by the Hunter process is deemed superior to the Kroll sponge because the reflux action of Na tends to wash the reactor walls free of titanium metal, thereby minimising contamination by iron and other elements in the retort materials of construction (Gambogi & Gerdemann, 1999).

The Kroll process has gained wider industrial acceptance and accounts for 99% of the global sponge supply due to the Mg economics, which render Mg a cheaper reducing metal (Nagesh et al., 2008). The ease of recycling $MgCl_2$ to regenerate Mg and chlorine gas, as shown in Figure 2.1(b), is also a contributing factor for the commercial domination of the Kroll process (Van Vuuren, 2009). However, speciality industries continue to use the Hunter process to produce high purity titanium (Gambogi & Gerdemann, 1999).

After refining to remove by-products (to be discussed in Section 2.5), the titanium sponge produced by both the Kroll and Hunter processes is used as a precursor in all downstream processes to produce titanium powder, as illustrated in Figure 2.2.

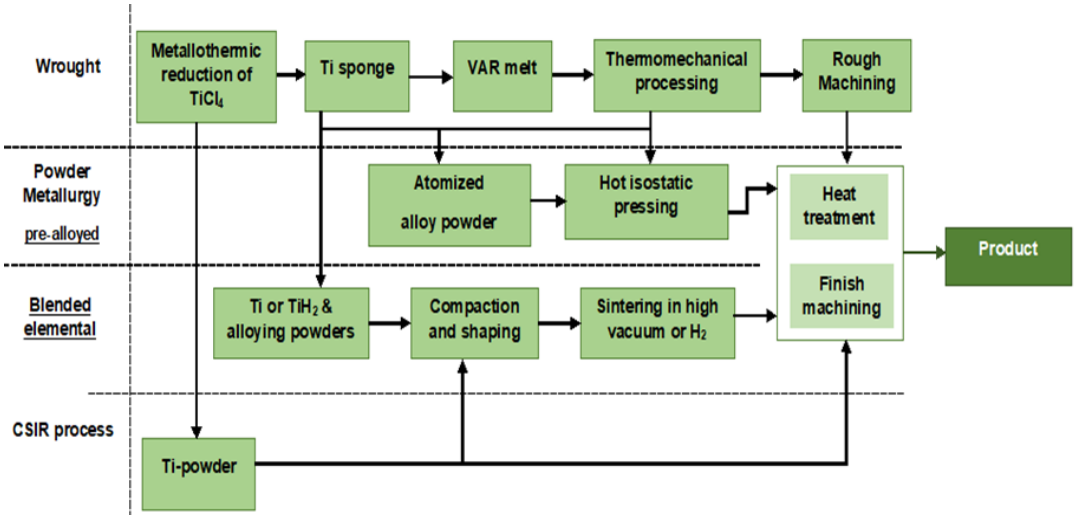

Figure 2.2 Block diagram summarising current titanium metal production process steps, including the CSIR-Ti process. Diagram adapted from Fang et al. (2018).

Presently, angular titanium powder is produced by the reversible hydride-dehydride (HDH) process, in which a titanium-containing precursor of sponge, billet, scrap or machining chips is heated in hydrogen to form brittle titanium hydride. This is subsequently pulverised, classified and reconverted to titanium metal powder by removing hydrogen in a vacuum annealing furnace (Froes & Imam, 2010; Van Vuuren et al., 2011). The powder is also processed from mill forms produced by melt refining and wrought processing of billet, scrap or machining chips. Well-established secondary or tertiary routes for producing powder from the sponge or milled products are gas atomisation and plasma rotating electrode processes (Sun et al., 2017).

Metal powders produced by these methods are expensive because they add cost to existing material costs by converting titanium products from conventional wrought processes into powder (Van Vuuren et al., 2011).

2.3 Justification for establishing a titanium industry in South Africa

South Africa is a country with abundant titanium ore reserves and has the sixth-largest ilmenite deposits after Australia, China, India, Brazil, and Norway (U.S Geological Survey, 2020). It also accounts for the third-largest rutile deposits after Australia and India (U.S Geological Survey, 2020). From 2015–2018, South Africa accounted for 36% of the global titanium feedstock exports (U.S Geological Survey, 2020). However, it can be argued that the local beneficiation of this resource is not capitalised as it is only concentrated and exported as low-value commodity TiO_2–

rich slag (Oosthuizen & Swanepoel, 2018). For instance, slag sells for 1–2 $/kg while an ingot of titanium metal costs 20–80 $/kg, and high-end products such as implants cost 10–1000 times more, implying that South Africa only realises 5% of the estimated $9 billion pigment industry (Chown, 2016; Oosthuizen & Swanepoel, 2018). Thus, by exporting titanium as slag, South Africa is not benefiting from this value-added market price increase. Owing to this fact, the development of a titanium value chain has been identified as a potential key growth area for South Africa (Chown, 2016; Oosthuizen, 2011). Consequently, a beneficiation strategy document for the minerals industry in South Africa was launched by the Department of Mineral Resources (Oosthuizen, 2011).

The strategy document identified the development of human capacity in titanium manufacturing and commercialisation of technologies to compete cost-effectively in international titanium markets as the primary key points that South Africa had to address to realise this objective (Oosthuizen, 2011). To meet the objectives set out by the strategy document, the Titanium Centre of Competence, hosted by the CSIR in collaboration with six local universities, was established by the Department of Trade and Industry (Chown, 2016).

Given the task to continually develop and commercialise technologies to compete cost-effectively in local and international titanium markets, CSIR established a comparative framework. The comparative framework was used to evaluate and screen current and alternative titanium production processes, including future industry projections, to establish a rational basis for selecting a given processing route, or combination of routes, to pursue in the field of primary titanium technology (Van Vuuren, 2009).

The framework revealed that the leading method for machining components in the industry is through ingot metallurgical techniques. Research and development work in the titanium industry over the years has been directed towards cost reduction to increase the titanium industry market share (Froes & Imam, 2010; Van Vuuren, 2009). These included finding alternatives or lowering the cost of ingots cast from vacuum arc re-melting (VAR) sponge, precursors, billets, slabs and fabrication routes (Froes & Imam, 2010). It was also revealed that continuing advances in the field of PM were generating increased interest in the direct production of near net shape and three-dimensional components from powder or wire feedstocks (Qian et al., 2010). Hence, PM technology has the potential to eliminate machining and reduce material losses during parts production resulting in downstream cost savings. In addition, the operating conditions required in PM are not as demanding as required for ingot production, such as the expensive skull melting

techniques used to minimise the reaction of molten titanium and crucibles during shape casting (Qian et al., 2010; Van Vuuren, 2009). PM techniques were identified as a promising avenue to low-cost titanium products. However, despite the advances made by PM to provide the impetus to broaden the use of titanium and titanium alloy powder, the universal challenge is still the availability of low-cost quality powder (Crowli, 2003; Peter et al., 2012; Qian et al., 2010).

Following considerations of the framework and critical evaluation of the various process routes to produce primary titanium metal, it was concluded that the most promising emerging primary powder technologies are those that can produce titanium powder directly (melt-less powder) at a cost comparable with that of sponge (Van Vuuren, 2009).

2.4 CSIR titanium powder process technology

The CSIR Primary Processes research group has been involved in developing a novel titanium powder process over the last decade. The patented process is commonly referred to as the CSIR-Ti powder process (Oosthuizen & Swanepoel, 2018; Van Vuuren & Oosthuizen, 2014). In this process, titanium metal is produced by reducing $TiCl_4$ with Li in a LiCl salt medium under Ar gas at a process temperature of 650°C, in a continuously stirred tank reactor (CSTR) configuration, as illustrated by the block flow diagram in Figure 2.3.

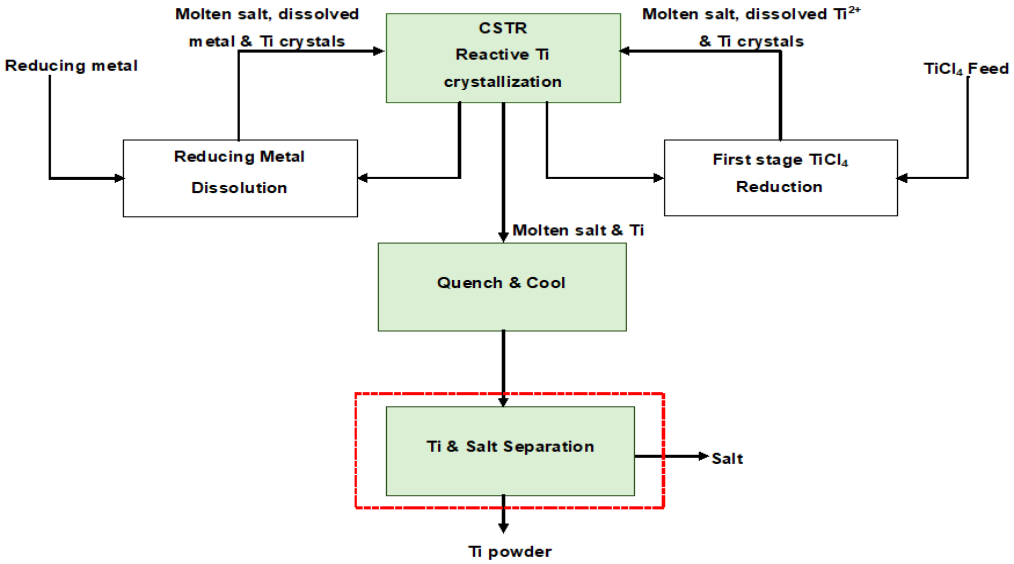

Figure 2.3 Block flow diagram of the CSIR-Ti process, indicating the three main process units and two sections for feed preparation (Oosthuizen & Swanepoel, 2018).

The configuration comprises three main units: CSTR reactive Ti-crystallisation, quench or cooling section, and Ti or salt separation stage. The CSTR reactive Ti-crystalliser is the central unit in which the lithiothermic reduction takes place. The unit consists of two additional sections for feed preparation: first-stage $TiCl_4$ reduction and reducing metal dissolution sections, with all sections controlled at a temperature of 650°C and operated simultaneously. In the first-stage reduction zone, $TiCl_4$ is reduced with a sub-stoichiometric mixture of Li and Ti powder in LiCl salt recycled from the CSTR reactive Ti-crystallisation unit to produce $TiCl_2$ dissolved in salt according to equation [2.8]. The $TiCl_2$-rich slurry thus produced is transferred to the CSTR reactive Ti-crystallisation section.

$$TiCl_4(s) + Li/Ti(l) \text{ in } LiCl \rightarrow 2\ TiCl_2(l) + LiCl(l) \qquad [2.8]$$

In the reducing metal dissolution zone, molten Li is dissolved into a slurry stream of LiCl-Ti recycled from the CSTR reactive Ti-crystallisation zone or fresh LiCl salt (at the start of the process). The Li-dissolution reactor comprises three dissolution vessels arranged in series to increase the residence time. Molten lithium (at approximately 250°C) is pumped into the first vessel preloaded with a recycled slurry stream from the CSTR reactive Ti-crystallisation section. The Li dissolves in the LiCl, and the molten slurry overflows to the second dissolution vessel where further dissolution of the Li occurs. The slurry overflows to a final dissolution vessel where any remaining Li metal is dissolved before overflowing to the CSTR reactive Ti-crystallisation zone.

Finally, in the CSTR reactive Ti-crystallisation zone, the two incoming streams are mixed with a high-intensity mixer to achieve rapid reagent dispersion and to reduce reagent supersaturation. The recycle stream is split to feed the two feed preparation sections, from where the streams return to the CSTR with low concentrations of reagents. This allows the final metallothermic reduction of dissolved $TiCl_2$ with dissolved Li to produce titanium metal powder and LiCl according to equation [2.9]:

$$TiCl_2 \text{ in } LiCl(l) + 2\ Li \text{ in } LiCl(l) \rightarrow Ti(s) + 2\ LiCl(l) \qquad [2.9]$$

The resulting crude product comprising titanium metal powder and LiCl exits from the CSTR reactive Ti-crystallisation zone into the cooling and quenching section. After cooling, the by-products and salt impurities must be separated from the metal powder (discussed in Section 2.5).

The low operating temperature afforded by the process chemistry provides the potential to minimise undue alloying of titanium with iron to form ferrotitanium (FeTi), as experienced in the Kroll process. It also offers the possibility to yield a higher purity product without contamination from products formed from corrosion of the retort construction materials. Furthermore, the temperature difference between Li boiling point (1330°C) and LiCl melting point (610°C), when compared with those of Na (b.p. 883°C) and NaCl (m.p. 801°C), is wide enough to ensure a more effortless process handling and safe operation. The process also has the potential to eliminate some of the downstream processing costs and steps associated with re-melting and milling titanium necessitated by conventional ingot metallurgy. Cost reduction using commercially available powder production methods is also envisaged because many titanium components could be fabricated directly using PM techniques, as illustrated in Figure 2.2.

2.5 Crude product purification methods and recovery

After completing the metallothermic reduction process, the resulting crude titanium sponge or powder is intermingled with excess Li, $TiCl_2$, $TiCl_3$ and LiCl salt by-product in quantities postulated in Table 2.1.

Table 2.1 By-product compositions in crude titanium sponge and powder—comparison of commercial Hunter/Kroll processes and CSIR-Ti process. Adapted from Garmata et al. (1970)

Process		Reductant in the salt	Sub-chloride	By-product salt
	Ti	Na, Mg or Li	$TiCl_2$ and/or $TiCl_3$	$MgCl_2$/NaCl/LiCl
		(mass%)		
Kroll[(a)]	50–70	30–35	0	15–20
Hunter[(a)]	15–25	0.1–1.0	0.1–3.0	75–85
CSIR-Ti[(b)]	22	0.5	2	78

[(a)] Kroll and Hunter data referenced from (Garmata et al., 1970). However, some sources state different quantities (Aleksandrovskii et al., 1982; Gambogi & Gerdemann, 1999); these quantities are thus for illustrative purposes only.

[(b)] Material balance of the CSIR-Ti processing units was used to collect the data.

The main difference between Kroll- and Hunter-produced crude sponges as shown in Table 2.1, is that the former has high Mg and $MgCl_2$ content, and no of $TiCl_2$ or $TiCl_3$. The latter contains $TiCl_2$ and $TiCl_3$ present in the crude product in complex-salt form and about 0.1%–1.0% unreacted Na metal dissolved in NaCl, despite completing the metallothermic reduction step with excess $TiCl_4$ (Aleksandrovskii et al., 1982; Garmata et al., 1970). This anomaly is a consequence of the

exothermic nature of the process, which renders it impossible to agitate the mass during the metallothermic reduction (Aleksandrovskii et al., 1982).

The CSIR-Ti process and the Hunter process are similar as they both contain copious salt by-product and excess titanium sub-chlorides. However, the only sub-chloride species in the CSIR-Ti process is $TiCl_2$ (due to the incorporation of the first-stage $TiCl_4$ reduction unit in Figure 2.3).

To obtain commercially pure (CP) titanium powder or sponge, the residual by-products must be separated and the content reduced to below appreciable levels, as specified in the ASTM B299 standard for grade 1–4 unalloyed titanium sponge. The methods for separating by-products and refining metal powder or sponge are divided into two types, namely; phase transition and physical separation techniques. Physical separation techniques include decanting, settling or filtration, and are cheaper than processes involving phase transitions, such as vacuum distillation and leaching (Van Vuuren, 2009). However, physical separation processes are insufficient to achieve stringent titanium product specifications (Van Tonder, 2010; Van Vuuren, 2009). Consequently, aqueous leaching and vacuum distillation are the only purification techniques that are used industrially to purify crude titanium (Poulsen & Hall, 1983; Van Vuuren, 2009).

2.5.1 Vacuum distillation

Vacuum distillation is a purification technique used to separate chloride by-products from the crude titanium sponge produced by the Kroll process. This is mainly because the recovery of Mg and $MgCl_2$ by alternative processes, i.e., leaching, has proven to be challenging due to a loss of the excess Mg (about 30%) given the insolubility of Mg in water (Gambogi & Gerdemann, 1999). This technique is based on the fundamental basis of exploiting the difference in vapour pressure of chloride by-products in the crude product over different temperature ranges (Liang et al., 2020, 2019).

In the latest Kroll process plants, metallothermic reduction and the subsequent vacuum distillation operations are confined to a closed-loop (single station) operation called the combined process (Nagesh et al., 1994). The combined process results in the advantage that the exothermic heat released during metallothermic reduction is harvested for re-use in the vacuum distillation step. The vacuum distillation process is operated at a temperature between 850–1000°C and a vacuum pressure of 0.1 Pa (Liang et al., 2018; Nagesh et al., 1994). This temperature range is similar to those used for metallothermic reduction (Habashi, 1997).

The configuration also eliminates the intermittent step of cooling the crude product, opening the reactor, reloading the batch into the vacuum distillation unit, reheating and soaking, as was required by the older conventional configurations (Gambogi & Gerdemann, 1999; Nagesh et al., 2008). Impurities are removed in situ, thus minimising sponge contamination by air (Yu & Jones, 2013). Simultaneously, the excess Mg and chloride by-products are recycled in an anhydrous form at high concentrations (Nagesh et al., 2008).

Sponge produced by this technique has low interstitial inclusions (oxygen and nitrogen) and is generally considered premium quality (Liang et al., 2018). However, the downside trade-offs of this technique include the exorbitant amounts of capital required to purchase expensive, sophisticated reactors that can withstand high vacuum at high temperatures (Nagesh et al., 1994). The technique also requires auxiliary equipment such as vacuum pumps, instrumentation controllers and software to prevent distillation channel blockages by condensation of the volatiles (Nagesh et al., 1994).

The slow nature of the batch process emanating from the inefficient heat transfer in vacuum also requires extremely long heating times; for example, it takes up to 48 h to vacuum distil 30%–35% of the residual $MgCl_2$ remaining in the titanium sponge. This implies that when the production yield increases, it will become challenging to control the heat balance and almost double the time will be required for processes that do not incorporate tapping as part of the metallothermic reduction.

Thermodynamic analysis is usually conducted to evaluate the possibility of separating by-products from Ti-powder using vacuum distillation. This is done by calculating the vapour pressures; a method considered an adequate theoretical approach for conducting preliminary analysis on the probability of volatilising by-products (Liang et al., 2020). To evaluate the possibility of separating CSIR-Ti by-products from the Ti-powder using vacuum distillation, the thermodynamic analyses conducted by Liang et al. (2019) and Van Vuuren (2009) were adapted to include Li and recalculated using constants from Gale and Totemeier (2004) to ensure consistency.

The vapour pressures were calculated using equations [2.10] for metals and [2.11] for halides, as recommended in Gale and Totemeier (2004) and compared against the Kroll process chloride by-products.

$$\log p = -A/T + B + C\log T + 10^{-3}DT \qquad [2.10]$$

$$\log p = A/T + B + C\log T + 10^{-3}DT \qquad [2.11]$$

where P is the vapour pressure of pure substances, in mmHg (133.32 pa); A, B, C, and D, are evaporation constants, and T is the absolute temperature in K.

Table 2.2 lists the evaporation constants of the main substances in crude titanium from both the Kroll and CSIR-Ti processes.

Table *2.2* Evaporation constants of the main substances in crude titanium sponge (Gale & Totemeier, 2004)

	A	*B*	*C*	*D*	Temperature (K)
Li	8415	11.34	−1.00	–	m.p.–b.p.*
Mg	7780	11.41	−0.86	–	298–m.p.
LiCl	−10760	22.30	−4.02	–	m.p.–b.p.
$MgCl_2$	−10840	25.53	−5.03	–	m.p.–b.p.
$TiCl_2$	−15230	19.36	−2.51	–	298–m.p.
$TiCl_3$	−9620	21.47	−3.27	–	298–m.p.

*m.p. : melting point; b.p. : boiling point.

Given these constants, the vapour pressures of all by-products were calculated and are presented in Figure 2.4.

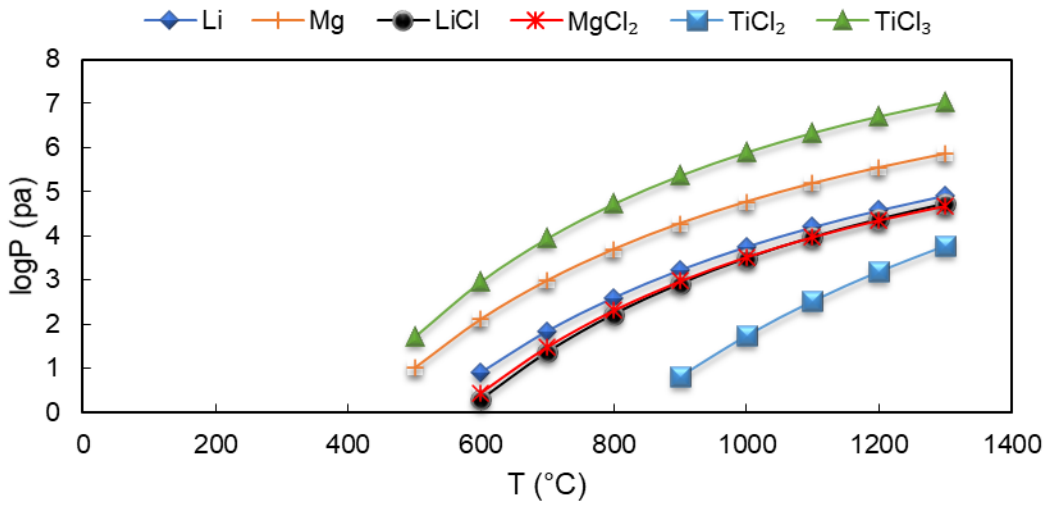

Figure 2.4 log *P*-*T* graph comparing the main by-products in the Kroll and CSIR-Ti processes, calculated from data in Table 2.2. Adapted from Liang et al. (2019) and Van Vuuren (2009).

As shown in Figure 2.4, the vapour pressures of LiCl and $MgCl_2$ at temperature ranges between 850–1000°C are almost the same. The vapour pressures of LiCl, $TiCl_2$, $TiCl_3$, $MgCl_2$, Li and Mg are all positive. On the contrary, Li is less positive than Mg due to its high boiling point of 1347°C vs. 1091°C. Hence, better separation of Mg is expected at the vacuum distillation operating temperatures. The volatilisation order in the CSIR-Ti processes is in the order $TiCl_3$, Li, and LiCl followed by $TiCl_2$. Furthermore, it is postulated that, under vacuum, the volatilisation temperature will be reduced, and the rate improved. The theoretical analysis indicates that CSIR-Ti crude product is amenable to purification by vacuum distillation.

2.5.2 Aqueous leaching

Aqueous leaching is an alternative separation and purification technique used to separate by-products from crude titanium sponge or powder. It has the advantage that the equipment required is much simpler and readily available, as most are already manufactured for other applications. The process can either be operated batch-wise or continuously and is usually conducted at low or ambient temperature conditions. Consequently, the initial and operating capital required is usually lower in contrast to vacuum distillation (Gambogi & Gerdemann, 1999; Garmata et al., 1970).

In the aqueous leaching technique, by-products are removed by selective dissolution in an active leaching solution. The simple theoretical analysis that can be used to establish whether aqueous leaching is amenable or not, is solubility; however, the recovery of the anhydrous halide salt is another equally key factor considered when considering the feasibility of applying this technique. For instance, the solubility of $MgCl_2$ in water (54.25 g/100 cm^3 at 25°C) is high; however, anhydrous $MgCl_2$ cannot be recovered from hydrated magnesium chloride (Van Vuuren, 2009). When $MgCl_2$ is evaporated under normal conditions, magnesium oxide (MgO) forms, necessitating the expensive step of dehydrating $MgCl_2 \cdot H_2O$ in hydrochloric acid (HCl) atmosphere (Van Vuuren, 2009). As a result, the leaching of Kroll-produced sponge is no longer practised industrially; however, crude sponge produced by sodiothermic reduction is exclusively purified by leaching because NaCl has a high boiling point (1465°C), which renders vacuum distillation difficult and uneconomical (Jamrack, 1963; Van Vuuren, 2009).

The aqueous leaching of by-products in crude titanium is conducted using acid as a lixiviant. The acid is used to circumvent the formation of insoluble hydrolysis products (hydroxides or oxychlorides), a consequence of the reaction between the sub-chlorides contained in crude titanium (Table 2.1) and water or alkaline solutions according to equations [2.12] to [2.15] (Jamrack, 1963):

$$6\ TiCl_2(s) + 6\ H_2O(l) \rightarrow 4\ TiCl_3(aq) + 2\ Ti(OH)_3(s/aq) + 3\ H_2(g) \quad [2.12]$$

$$Ti^{3+}(aq) + 2\ H_2O(l) \rightarrow TiO_2(s) + 4\ H^+(aq) + e^- \quad [2.13]$$

$$TiCl_2(s) + 12\ H_2O(l) \rightarrow 2\ [Ti(H_2O)_5(OH)]Cl_2(s/aq) + H_2(g) \quad [2.14]$$

$$TiCl_3(s) + 2\ H_2O(l) \rightarrow TiO_2(aq) + 3\ HCl(aq) + 1/2\ H_2(g) \quad [2.15]$$

The insoluble hydrolysis products precipitate in the pores of the sponge and are passed into the sponge as an oxide, thus contributing to the total oxygen content (Jamrack, 1963; Kelly, 1963). However, in the presence of an acid, the sub-chlorides dissolve and stay in solution (Boozenny et al., 1961). In addition to preventing insoluble hydrolysis products from forming, the acid also neutralises NaOH from excess Na metal and water reaction.

The acids employed for the leaching process include 0.16 M–0.48 M HCl, sulphuric acid, acetic acid, aqua regia and 0.45 M nitric acid (HNO_3) solutions (Aleksandrovskii et al., 1982; Choi et al., 2019; Garmata et al., 1970; Kohli, 1981).

2.5.3 Plant practice: Hunter-produced sponge leaching procedure

In commercial operation of the Hunter process, the feed preparation process entails cooling down the retort after reduction, extraction of the crude sponge from the reduction retort by mechanical means, such as boring or extrusion (Garmata et al., 1970), followed by crushing with a hammer mill into small chips with a particle size ranging from 3–10 mm (Garmata et al., 1970; Poulsen & Hall, 1983). The crude sponge is crushed to maximise the surface area exposed to the leaching liquor because it is practically impossible to remove by-products trapped in closed pores within the dendritic sponge morphology.

Acid leaching is carried out either in a semi-continuous or a two-stage batch type process, in an open-type rubber-lined steel vessel fitted with a stirrer and an exhaust for releasing gases (Garmata et al., 1970). Each steel vessel is fitted with a plastic filter medium at the base to ensure that the residual sponge remains in the vessel throughout the leaching cycle (Garmata et al., 1970; Jamrack, 1963). Furthermore, the leaching vessel is fitted with a false bottom and valve underneath for draining the salt solution and for maintaining a constant leach liquor level. Hence ensuring that salt is drained at the same rate as the rate at which fresh leach liquor is added to ensure steady-state conditions in the system (Jamrack, 1963).

In the batch-type leaching process, the first-stage leaching is conducted for 30–60 min and the second stage for 60–120 min. The temperature in the leaching vessel is maintained at 20–30°C by ensuring thorough agitation. The dissolution of NaCl is endothermic (+3.9 kJ/mol); thus, no cooling is required during leaching (Garmata et al., 1970). The leaching reagent consists of 0.33 M HCl in the first stage and 0.16 M HCl in the second stage, at a solid:liquid ratio of 1:4 (Garmata et al., 1970). Acid leaching is followed by washing and drying by thermal, vacuum drying, mechanical centrifuge or a combination of these methods (Poulsen & Hall, 1983).

2.6 Crude CSIR-Ti purification process selection and justification

Based on the preliminary thermodynamic analysis shown in Figure 2.4, it is apparent that the crude product from the CSIR-Ti process can be purified by vacuum distillation. However, as discussed, the technique is much slower, with implications that the CSIR-Ti crude product will require more residence time to distil the LiCl effectively. Moreover, studies by Hansen and Gerdemann (1998) revealed that the high-vacuum distillation temperature tends to sinter the powder, thus altering the resulting powder morphology.

Considerations of LiCl solubility in water (63.7 g/100 cm^3 at 25°C) revealed that the by-products in the CSIR-Ti crude product are amenable to aqueous leaching; additionally, large quantities of salt will be easily removed by aqueous leaching without sintering the titanium particles (Van Vuuren, 2009). The recovery of LiCl from the resulting brine or leach liquor is relatively easy (Gambogi & Gerdemann, 1999).

Leaching has the disadvantage that it inevitably creates a surface oxide layer due to exposure of the titanium surface to the water-containing leaching solvent. This was proven by electrochemical studies to ascertain the behaviour of titanium in non-aqueous media, where it was found that titanium cannot be passivated by anodic polarisation in acidic methanol solutions and other media

unless small quantities of water were added in the non-aqueous solution (Menzies & Averill, 1968). This implies that oxide layer formation is inherent to leaching and the surface oxide layer will contribute to the oxygen content.

However, Hansen and Gerdemann (1998) and Van Vuuren et al. (2011) indicated that the effects of the passive oxide layer could be reduced by increasing the powder particle size to achieve a favourable surface-to-volume ratio. The most suitable purification process was thus selected based on preliminary selection criteria, which included nature and quantity of the by-products in Table 2.1, advantages and disadvantages of each technique, capital and operating costs. Based on these factors, it was concluded that acid leaching was the purification process more suited to the CSIR-Ti process, as it aligns with the objective of intending to find alternative techniques to produce cost-effective primary titanium powder.

2.7 Preliminary lixiviant selection

The crude CSIR-Ti product will thus be purified by a series of chemical leaching steps to separate the by-products; however, a suitable lixiviant must be selected for this processing step. In titanium metallurgy, by-products determine the leaching conditions and lixiviant because the side reactions of excess Li and $TiCl_2$ complicate leaching by contaminating the titanium metal, as demonstrated by equations [2.12] to [2.15].

Lithium is stable and does not burn spontaneously in air or water. However, it reacts violently with inorganic acids (Jeppson et al., 1978). The neutralisation reaction of Li yields aqueous lithium hydroxide (LiOH(aq)) dissolved in solution according to equation [2.16] (Jeppson et al., 1978). The LiOH(aq) results in increased pH which favours the precipitation of the hydrolysis products, as discussed further in Section 2.8.2.

$$2\,Li(s) + 2\,H_2O(l) \rightarrow 2\,LiOH(aq) + H_2(g) \qquad [2.16]$$

A suitable lixiviant should selectively dissolve and neutralise all the by-products without contaminating the titanium metal product. In general, the leaching lixiviants and schemes proposed in the literature can be classified into two schemes:

1. Acidic leaching using a non-oxidising acid: dilute HCl (Garmata et al., 1970).
2. Acidic leaching using an oxidising acid: dilute HNO_3 (Jamrack, 1963).

Leaching schemes that involve the addition of small quantities of oxidising agents (such as nitric or ferric chloride, sodium or potassium nitrate, hydrogen peroxide and oxidising gases such as oxygen chlorine and ozone) into the acids to prevent hydrogen evolution and absorption thereof have been proposed (Boozenny et al., 1961; Choi et al., 2019; Gambogi & Gerdemann, 1999; McKinley, 1955). Additions of inhibitors and complexing agents into the acid solutions to prevent the dissolution and oxidation of the Ti-sponge have also been previously proposed (Boozenny et al., 1961; McKinley, 1955). However, in almost all these suggestions, the inventors could not describe the reaction mechanism by which the tendency for the oxidation of the cations to a higher valent state and the consequent evolution of hydrogen is prevented (Garmata et al., 1970; Kelly, 1963). Almost all the alternative leaching schemes suggested in these patents were concerned with counteracting the absorption of hydrogen by Ti-sponge or powder metal than optimising the process of leaching to ensure that all the impurities were within acceptable limits.

Recent studies have indicated that although hydrogen absorption embrittles titanium metal, its absorption is completely reversible as the gas can be readily removed by heating in a high vacuum or under Ar as applied in the HDH powder production process (Choi et al., 2019; Goso & Kale, 2011). Furthermore, the proposed leaching processes are complicated. Consequently, only the possibility of using HCl and HNO_3 was evaluated, as there is enough circumstantial evidence to prove that both acids are effective in counteracting the hydrolysis reaction posed by the sub-chlorides even without inhibitors. It must be noted that in this study the literature assessment of the possibility of using HNO_3 as a lixiviant was only investigated for comparison purposes, no experimental work was undertaken.

For the selection of a suitable acid, the following essential factors were taken into consideration as recommended in Habashi (1999); namely, whether the products after the leaching process will be separable and the spent acid efficiently or economically recovered for recycling, the cost of purchasing the lixiviant, inclusive of corrosivity and ease of handling.

The probable overall reactions between dilute HCl and HNO_3 with Li and $TiCl_2$ yield the products shown in equations [2.17] to [2.20]:

$$2\ Li(s) + 2\ HCl(aq) \rightarrow 2\ LiCl(aq) + H_2(g) \qquad [2.17]$$

$$2\ TiCl_2(s) + 2\ HCl(aq) \rightarrow 2\ TiCl_3(aq) + H_2(g) \qquad [2.18]$$

$$8\ Li(s) + 10\ HNO_3(aq) \rightarrow 8\ LiNO_3(aq) + NH_4NO_3(g) + 3\ H_2O(l) \quad [2.19]$$

$$TiCl_2(s) + 2\ HNO_3(aq) \rightarrow Ti(NO_3)_2(aq) + 2\ HCl(g/aq) \quad [2.20]$$

By just considering the reaction products formed in dilute solutions of both HCl and HNO_3 equations [2.17] to [2.20], it can be noted that HCl is a common chemical reagent (it contains chlorine as a common ion). Thus, it does not contribute any foreign ions into the system because even the solvation of the lithium chloride salt by-product yields LiCl(aq). This simplifies downstream purification in contrast to HNO_3, which produces aqueous lithium nitrate, and has implications that the downstream crystallisation system will have to be adapted to handle the new compound.

The major advantage of using HCl as a leaching agent is its cost, which is the lower of the two mineral acids suggested, as shown in Table 2.3. It is believed that leaching with HCl is much simpler, unlike other processes that utilise complex experimental variants (Choi et al., 2019). Given these factors, HCl was expected to be a promising leaching agent in the present study.

Table 2.3 Comparison of selected acid lixiviants

Category	Price as of 01 August 2020	Corrosivity
HCl (32%)	R 700 for 25 L, from Merck (Pty) Ltd South Africa	Very corrosive, equipment must be rubber-lined or manufactured by physical vapour deposition (carbon filled), polytetrafluoroethylene, viton or ceramic magnet.
HNO_3 (65%)	R 4500 for 25 L, from Merck (Pty) Ltd South Africa	Very corrosive, equipment must be rubber-lined or manufactured with polytetrafluoroethylene, stainless steel 303/304, titanium, hastelloys or alumina ceramic.

2.8 Operating parameter selection and behaviour of impurities

Aqueous leaching of titanium is termed chemical leaching. Thus, the leaching condition boundaries should be selected such that the titanium metal sponge or powder is not dissolved nor contaminated during acid leaching of the by-products. It has been established that, despite the high chemical stability of compact titanium, titanium sponge and powder are soluble in HCl solutions due to their large specific surface areas (Garmata et al., 1970).

Titanium solubility is more prominent in HCl concentrations greater than 1 M, wherein titanyl ion, TiO^{2+} (colourless), and titanous ion, Ti^{3+} (violet), are the dominant species, as demonstrated in the titanium Pourbaix or Eh–pH diagram as indicated in Figure 2.5 (Sole, 1999; Zhu et al., 2011). However, Straumanis and Chen (1951) acknowledged that while titanium metal is soluble in dilute HCl solutions, the dissolution occurs with difficulty, is extremely low and is affected by impurities. As a result, it is reported that only 0.5% titanium sponge or powder dissolves in 0.16–0.33 M HCl solutions at a temperature of 100°C (Garmata et al., 1970).

The slow dissolution is attributed to the stable passivated $TiO_2 \cdot H_2O$ that forms in the aqueous medium in the absence of a complexing agent, as illustrated in Figure 2.5. The passivated $TiO_2 \cdot H_2O$ is the dominant species in water and its range of stability can be expanded into aqueous reducing acid media (pH 6–2.5) (Figure 2.5) (Pourbaix, 1974). According to Zhu et al. (2011), $TiO_2 \cdot H_2O$ precipitates at pH ranges greater than 5. At higher pH (pH ≥ 12), $TiO_2 \cdot H_2O$ goes into solution and titanate ions ($HTiO_3^-$) become the dominant species. The optimal cut-off pH range is between 0 and 1.5 because in this pH range, Ti metal dissolution and $TiO_2 \cdot H_2O$ formation are at minimum. These pH ranges are in good agreement with recommendations by Seon and Nataf (1988) to use a pH of 1.5 for leaching lithiothermically produced crude titanium with HCl or HNO_3.

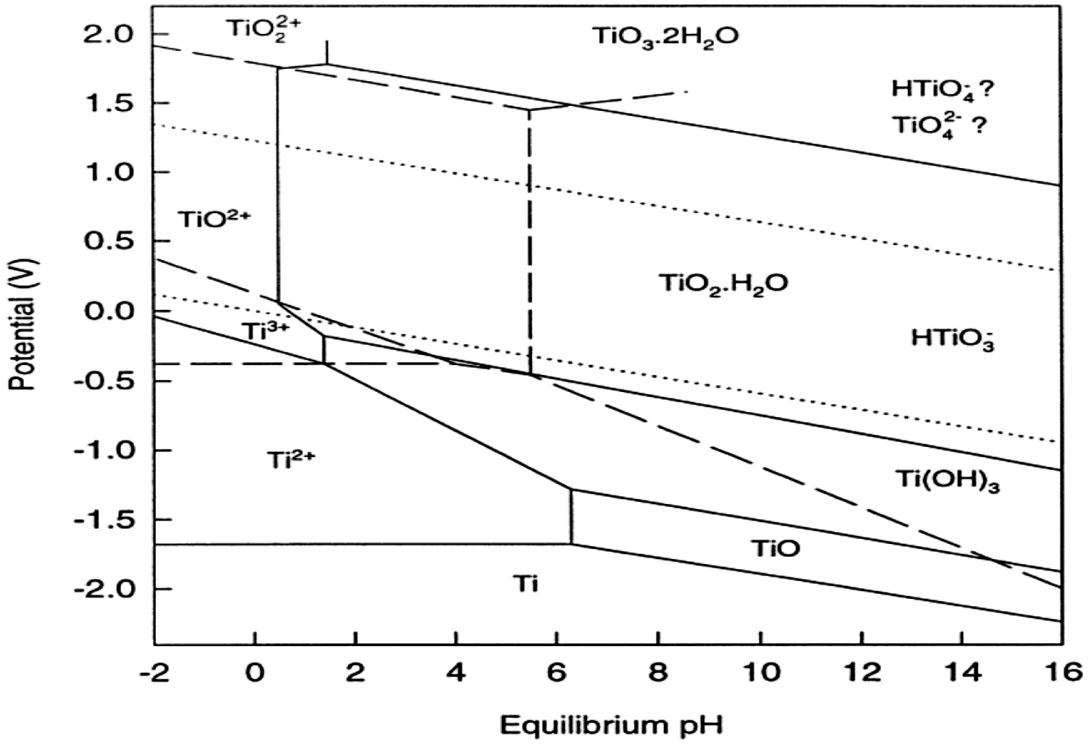

Figure 2.5 Eh–pH diagram for Ti-H_2O system (Pourbaix, 1974).

2.8.1 Aqueous chemistry ($TiCl_2$)

Even though titanium sub-chlorides in the crude product are present in complex-salt form, it is reported in Garmata et al. (1970) that these sub-chlorides react with aqueous solutions just like the individual sub-chlorides. However, the reaction is perceived to be slow, unlike that of the individual sub-chlorides. Consequently, the aqueous chemistry of the $TiCl_2$ present in the CSIR-Ti crude product is reviewed from that perspective. Little is published about the aqueous chemistry of the aqua titanium (II) cation (Ti^{2+}(aq)), due to its rapid oxidation in aqueous solutions, which occurs even at low pH (Cotton & Wilkinson, 1980; Gould, 2011). There have been reports that it exists for some time in ice-cold solutions of HCl, and further suggestions of its existence are provided by the electrode potential of Ti^{2+}/Ti^{3+} = −0.37 V vs. standard hydrogen electrode, which appears in most resources and the Pourbaix diagram in Figure 2.5 (Cotton & Wilkinson, 1980; Kölle & Kölle, 2003). What is known about Ti^{2+}(aq) was notably reported by Kölle and Kölle (2003), Park et al. (2012) as well as Yang and Gould (2005). Gould (2011) concluded that in all the reports confirming the existence of Ti^{2+}(aq), the samples examined contained both hydrofluoric acid and Ti^{4+} in highly acidic conditions, indicating that these contaminants might have stabilised Ti^{2+} ion in acidic media. This shows that, under different conditions, the transients might be short-lived.

However, it must be noted that Sekimoto et al. (2010) based their H_2 volumetric analysis and titration studies procedure on the theory that $TiCl_2$ reacts with 1 M HCl solution in a standard redox reaction to form titanous ions, Ti^{3+} (violet), and evolve H_2 in the absence of an oxidising agent according to equation [2.18] (Richens, 1997; Sekimoto et al., 2010; Wang et al., 2013).

2.8.2 Ti(III) aqueous chemistry—hydrolysis of Ti^{3+}

As the impurity with the direst consequences on the final product properties, the speciation of Ti(III) in HCl and stability thereof has direct implications for the probability of recovering the ion in its soluble state and consequently the selection of the leaching parameters and scheme. According to the Pourbaix diagram in Figure 2.5, Ti^{3+} ion is the predominant stable species under reducing conditions and pH ≤ 1. However, it must be noted that the ion can easily be oxidised by aerial oxidation to form tetravalent titanium(IV) TiO^{2+}, as shown in equation [2.21]:

$$4\ Ti^{3+}(aq) + O_2(g/aq) + 2\ H_2O(l) \rightarrow 4\ TiO^{2+}(aq) + 4\ H^{+}(aq) \qquad [2.21]$$

The rate of autoxidation in HCl is dependent on the volume of absorbed oxygen and the pH of the solution (Mackenzie & Tompkins, 1942; Yakovleva et al., 1974), so the rate of autoxidation is significantly retarded in highly concentrated acidic solutions (Ashton, 1977).

Even the existence of Ti^{3+} ion in the free state in aqueous solutions is a controversial issue, with reports predicting that, due to its relatively high ionic potential, it cannot exist in free form in aqueous solutions. Instead, it either oxidises or hydrolyses or forms hydrolysed polymeric species or complexes with various ligands, such as Cl^-, OH^-, CN^-, SO_4^{2-} and F^- (Ashton, 1977; Nabivanets, 1965). Some reports suggest that Ti^{3+} ion is a dominant species only in HCl solution of a pH ≤ 0.5 and that the main Ti(III) ionic species in dilute HCl solutions of pH up to 1 is the hexaquotitanium ion $[Ti(H_2O)_6]^{3+}$ (pale reddish-purple) (Cassaignon et al., 2007; Pecsok & Fletcher, 1962). The $[Ti(H_2O)_6]^{3+}$ has a measured *pKa* value between 1.8 and 2.5 (Cassaignon et al., 2007; Clark, 1973; Richens, 1997). Ti(III) is appreciably hydrolysed at pH ≥ 0.7 (Sole, 1999).

Prediction of predominating T(III) species in various pH ranges

A detailed study to investigate the chemistry of $Ti(H_2O)_6^{3+}$ in aqueous solutions was undertaken by Ashton (1977) using a combination of potentiometric titration, conductometric and spectrophotometric methods under an inert atmosphere of nitrogen gas bubbled to prevent aerial oxidation. The various species formed at different pH values were reported. Ashton (1977)

presented the rapid potentiometric titration data in Figure 2.6, which he classified into regions (a) primary hydrolysis and (b) secondary hydrolysis to represent the two stages of hydrolysis product formation. Region (a) was considered to be good evidence to prove that in HCl solutions and at low pH values, i.e., at 2 < pH < 4, the addition of base results in a ratio of Ti(III):OH^- of 1:1 (Ashton, 1977). Primary hydrolysis consequently yields the soluble monohydroxylated compound $TiOH(H_2O)_5^{2+}$ according to equation [2.22]:

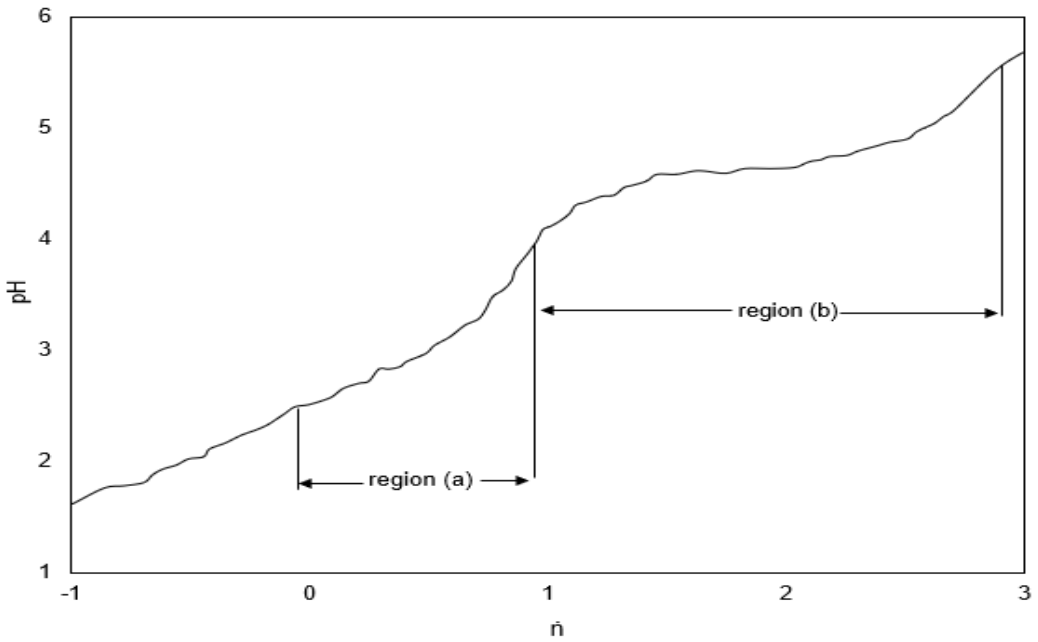

Figure 2.6 Rapid pH titration curve for 0.11 M Ti(III) (80 ml) with 1.97 M NaOH. $[Cl^-]$ = 0.45 M in the initial solution. $\bar{n}$ = ratio $[OH^-]$:[Ti(III)]. From Ashton (1977).

$$Ti(H_2O)_6^{3+}(aq) + OH^-(aq) \rightleftharpoons TiOH(H_2O)_5^{2+}(aq) \qquad [2.22]$$

Cassaignon et al. (2007) reasoned that the addition of a base in region (a) leads to the neutralisation of excess HCl and, consequently, the initiation of Ti(III) hydroxylation. It was also observed that an increase in pH corresponded with a colour change from a lighter to a darker violet shade (Ashton, 1977). These observations were attributed to co-ordination re-arrangement or bridging reaction to form a more stable species, such as the dimer $TiO(OH_2)_{10}^{4+}$ (Cassaignon et al., 2007). Quantitative studies have indicated that about 1% dimer was present at pH = 1 and 10% at pH = 3 (Cassaignon et al., 2007). However, Pecksok and Fletcher (1962) argued that all the polynuclear species in region (a) do not form to any appreciable extent and thus concluded that the only Ti^{3+} species at pH < 3 is $Ti(OH)^{2+}$.

Characterisation of the visible absorbance spectra indicated that the Ti(III) concentration is constant when the ratio of $[OH^-]$:[Ti(III)] is 1. After this, at slightly higher pH values, i.e., $4 \leq pH < 6$ (region (b) in Figure 2.6), the absorbance correspondingly increased owing to the formation of $Ti(OH)_3(s)$, a brown precipitate, due to the secondary uptake of additional OH^- according to reaction [2.23] (Ashton, 1977):

$$TiOH(H_2O)_5^{2+}(aq) + 2\ OH^-(aq) \rightleftharpoons Ti(OH)_3(s) + 5\ H_2O(s) \qquad [2.23]$$

It was also observed that adding more base changed the brown colour to black, followed by a rapid pH increment and a slow decrease back to pH 4.1 (Ashton, 1977). Similar behaviour and observations were reported by Pecksok and Fletcher (1962), who attributed the observation to the formation of hydroxo or oxo-groups in polynuclear species of the types indicated by reactions [2.24] and [2.25] (Ashton, 1977; Kelly, 1982; Pecsok & Fletcher, 1962):

$$Ti(OH)_3(s)\ (brown) \rightleftharpoons TiO(OH).\ nH_2O(s)\ (black) \qquad [2.24]$$

$$2\ Ti(OH)^{2+}(aq) \rightarrow TiOTiOH^{3+}(aq) + H^+(aq) \qquad [2.25]$$

The presence of oxo-group species was confirmed by adding a sodium tartrate solution, which turned the solution a stable black colour (Pecsok & Fletcher, 1962). The black precipitate was also readily oxidised from Ti(III) to Ti(IV) at pH > 5 to give a dark blue solution. Its stability is sensitive to chloride ion concentration and, as a result, it is only present in equilibrated solutions when minimum chloride ion concentrations are used (Ashton, 1977). It is further reported by Kelly (1982) that in notably less acidic media, the addition of a concentrated base (e.g. NaOH) changes the colour from dark blue to white. At these pH ranges, the rate of oxidation of Ti(III) ions in solution increases sharply and becomes dependent upon the stirring rate as the reaction passes from activation to mass transport control (Kelly, 1982), with reaction [2.26] becoming the rate-determining step. The observed pH decrease was attributed to the slow hydrolysis of a dimeric chloro primary hydrolysis species that supply H^+ ions in the same region after equilibrium (Richens, 1997).

$$(TiOH)^{2+}(aq) \rightarrow Ti^{4+}(aq) + e^- \qquad [2.26]$$

Although evidence obtained from the above studies managed to clarify the pH dependence of the hydrolysis products, the investigations were limited by the absence of non-complexing reagents.

This limitation was addressed by Mackenzie and Tompkins (1942), who considered a system with HCl solutions of various concentrations. They suggested that HCl addition retards the hydrolysis process by converting the pH-dependent hydrolysis product $Ti(OH)^{2+}$ to $TiCl^{2+}$ in proportion to the acid concentration. Also, they postulated that the reaction proceeds via two mechanisms that involve the pH-dependent hydrolysis reaction [2.27] and complex formation [2.28], a consequence of a direct dependence on the hydrogen ion concentration. If, however, the reversible reactions were simultaneously established, these two equilibria would correspond together to reaction [2.29] (Mackenzie & Tompkins, 1942; Shuvalov et al., 1978):

$$Ti^{3+}\ (aq) + H_2O\ (l) \rightleftharpoons (TiOH)^{2+}(aq) + H^{+}\ (aq) \qquad [2.27]$$

$$Ti^{3+}(aq) + Cl^{-}(aq) \rightleftharpoons TiCl^{2+}(aq) \qquad [2.28]$$

$$Ti(OH)^{2+}(aq) + HCl(aq) \overset{K_1}{\leftrightarrow} TiCl^{2+}(aq) + H_2O(l) \qquad [2.29]$$

These authors further concluded that $(TiOH)^{2+}$ is the oxidisable species; therefore, the addition of acid retards the reaction in proportion to the acid concentration (Mackenzie & Tompkins, 1942). This phenomenon was also reported by Ashton (1977), who noted that there was no evidence of oxidation in the primary hydrolysis region. The conclusions of Mackenzie and Tompkins (1942) were consistent with those by Cservenyak et al. (1995), who studied the ultraviolet (UV) absorption spectra of Ti(III) and also observed a decrease in absorbance of Ti^{3+} ions with time, a phenomenon they attributed to the absence of intramolecular charge transfer in the mixed oxidation state intermediate incorporating the chloride ion, which results in slow kinetics of Ti^{3+} oxidation in chloride media due to complexation reaction [2.30]:

$$Ti^{3+}(aq) + 12\ Cl^{-}(aq) + 2\ H_2O(l) + O_2\ (g/aq) \rightarrow 4\ [TiOCl_3]^{-}(aq) + 4\ H^{+}(aq) \qquad [2.30]$$

In highly concentrated HCl solutions with higher chloride ion activities up to 16 M HCl, the water molecules are substituted by chloride ions to form anionic complexes. Species of the type described by the general equation [2.31] and example [2.32] are dominant in these solutions (Cservenyak et al., 1996; Nicholls, 2017):

$$Ti(H_2O)_6^{3+}(aq) + n\,Cl^{-}(aq) \rightleftharpoons [Ti(H_2O)_{(6-n)}Cl_n]^{(3-n)+}(aq) + n\,(H_2O)\,(l) \quad [2.31]$$

$$Ti(H_2O)_6^{3+}(aq) + HCl\,(aq) \rightleftharpoons [Ti(H_2O)_5Cl]^{2+}(aq) + H_2O(l) \quad [2.32]$$

Based on equilibrium equations and constants reported, Cservenyak et al. (1995) calculated the $Ti(H_2O)_6^{3+}$ speciation with 0.1 M Ti(III) activity in 1 M HCl aqueous solutions, as shown in Figure 2.7.

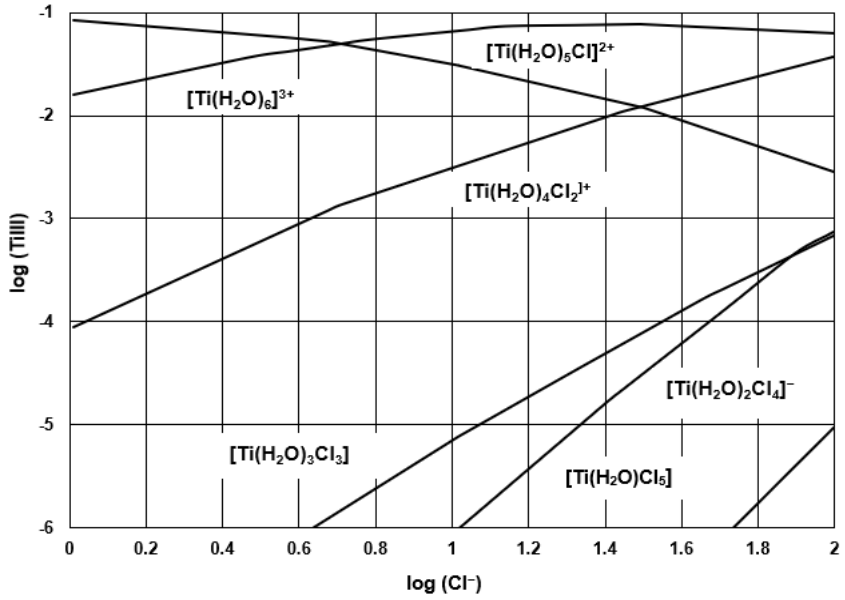

Figure 2.7 Speciation diagram for 0.1 M Ti(III) activity at 20°C taken from Cservenyak et al. (1995).

According to this diagram, $[Ti(H_2O)_5Cl]^{2+}$ or $TiCl^{2+}$ ions are the most predominant species in 1 M HCl aqueous solutions. However, reports indicate that these chloride ions complex weakly, unlike sulphate ions (Kelly, 1982).

The stability constants of the various probable hydrolysis and chloro-complexes shown in Table 2.4 indicate that the stability constant of $TiCl^{2+}$ is much lower than that of $TiOH^{2+}$. Nicholls (2017) argued that the complexes of Ti^{3+} and Cl^{-} do not form to any appreciable extent, but instead, the chloro-complexes depend on the acid concentration. The acidic solutions of Ti(III) salts in inert atmospheres (under nitrogen and argon) are relatively stable (Ashton, 1977).

Table 2.4 Stability constants for the speciation of titanium in HCl media

Reaction	Stability constant	Reference
$Ti(H_2O)_6^{3+}(aq) + HCl(aq) \rightleftharpoons [Ti(H_2O)_5Cl]^{2+}(aq) + H_2O(l)$	*K*sta = ≤ 0.1	(Shuvalov et al., 1978)
$Ti^{3+}(aq) + OH^-(aq) \rightleftharpoons (TiOH)^{2+}(aq) + H^+(aq)$	Log*K* = 11.5	(Sole, 1999)
$Ti(H_2O)_6^{3+}(aq) \rightarrow Ti(OH)(H_2O)_5^{2+}(aq) + H^+(aq)$	*K* = ca. 0.005	(Cotton & Wilkinson, 1980)
$Ti(OH)(H_2O)_5^{2+}(aq) + OH^-(aq) \rightleftharpoons Ti(OH)_3(s) + H_2O(s)$	log*K*sp=−32.19	(Ashton, 1977)
$Ti^{3+}(aq) + OH^-(aq) \rightleftharpoons (TiOH)^{2+}(aq) + H^+(aq)$	6.3×10^{-3}	(Kelly, 1982)

Lithium chloride, the main impurity in the CSIR crude product, is neutral and has the advantage that it will not interfere with the pH. The salt has been used to maintain ionic strength in electron spin resonance hydrolysis studies (Gardner, 1967; Shuvalov et al., 1978). However, excess Li is inherent to the CSIR-Ti process; consequently, the pH is expected to rise, as discussed in Section 2.7.

Lithium has a low co-ordination number, unlike $TiCl_2$, which explains its high reactivity (Clark, 1973). Hence, the presence of large quantities of Li will consume the acid, resulting in increased pH and the possibility of irreversible hydrolysis and secondary hydrolysis (Garmata et al., 1970; Shuvalov et al., 1978).

2.8.3 Temperature and effects thereof

The neutralisation of Li in water, equation [2.16], is highly exothermic, releasing energy up to $\Delta H^{\circ}_{sln} = -445.6$ kJ/mol (Monnin et al., 2002). The total amount of metal surface or the total number of metal atoms exposed to water at any instant will primarily control the rate of heat, assuming relatively little hinderance of Li metal–water contact due to hydrogen gas liberation (Jeppson et al., 1978).

It is imperative to prevent overheating of the solution and localised heating at the reaction-mass–solution interface to prevent oxidation of Ti powder or sponge, precipitation of hydrolysis products and the dissolution of titanium powder, as discussed in Chapter 1. A combination of suitable agitation and external cooling can be used to lower the temperature or alternatively reduce the feed rate and increase the solution volume. However, the latter alternative is not encouraged

because increasing the volume requires equipment of large capacity to handle the amount of process solution, thus resulting in reduced overall yield and production (Garmata et al., 1970).

2.9 Section summary

The work by Gould (2011), Ashton (1977), Cassaignon et al. (2007), Peckson and Fletcher (1962), Cservenyak et al. (1995) as well as Mackenzie and Tompkins (1942), in which the essential aqueous chemistry of Ti(III) in various mediums and pH conditions are described, are given in Sections 2.8.1 and 2.8.2, respectively. Their investigations indicated that multiple pH-dependent hydrolysis products are formed by Ti(III) in solution. They further revealed that the Ti(III) behaviour thereof is dependent on pH increase, which is a direct result of hydroxide ion concentration, agitation and initial metal ion concentration, as discussed in Section 2.8.2. In addition to this, the species produced were unstable and either formed solid hydroxide or oxide phase or continued to form stable species by bridging reactions or co-ordination re-arrangement.

Almost all these investigations were concerned with identifying the dominant species of Ti(III) ions and the extent of stability of either the complexes or hydrolysis products formed under various conditions inclusive of pH. However, given that the behaviour of the ions in solution, specifically the hydrolysis products formed, has a significant contribution to the impurities in the purified product, as discussed in Sections 2.5.2, 2.7 and 2.8, the solution chemistry is of significance to this study. Hence, thorough rationalisation of the main objective of making a product that is within specifications, as stated in Chapter 1, is dependent on chemistry. As a result, optimisation of acid leaching requires that the mechanism and chemical speciation in the solution be understood.

The Ti–H_2O Eh-pH diagram in Figure 2.5 provided the thermodynamic analysis information regarding the complexes formed, which is essential for understanding the Ti species redox and solubility behaviour. Given the preliminary details in this chapter and Ashton's conclusion that at pH less than 2, the addition of base to Ti(III) will still yield soluble species. It can be concluded that HCl as a lixiviant can be used with confidence, provided the maximum concentration is not above 1 M. The maximum pH should be maintained below 3 to prevent precipitation of secondary hydrolysis products. Given that most authors recommend the pH to be maintained between 1.5 and 2 (Jamrack, 1963; Seon & Nataf, 1988), the most probable operating pH will have to be selected within these constraints if the main objective stated in Chapter 1 is to be achieved.

3 EXPERIMENTAL METHODS AND MATERIALS

3.1 Overview

The effects of particle size, initial temperature and initial HCl concentration on the total residual chloride and oxygen contents of the CSIR-Ti product were investigated in this work. The initial HCl concentration was varied between 1 M and 0.032 M. The average particle sizes tested were divided into –10 mm and +10 mm while temperature ranges of 14–30°C and 30–60°C were examined. The size fraction range was selected based on the 3–10 mm used in the Hunter process (Garmata et al., 1970). The temperature range was selected to allow for maximum flexibility while preserving the integrity of the product, specifically the oxidation of titanium as discussed in Section 1.2.

The variable ranges were selected based on a two-level factorial experimental design strategy, an experimental design procedure that only considers extremities (minima and maxima) in the test parameters (Free, 2013; Montgomery, 2017). By only considering the extreme parameter values, the strategy has the advantage that a large number of variables, their interaction and the effect of each factor on the response output are investigated at the same time. Consequently, the factorial design experimental strategy keeps the number of trials to a minimum without sacrificing precision (Montgomery, 2017).

3.2 Materials

The crude titanium samples used for the test work were produced at the CSIR Titanium Pilot Plant in Pretoria, South Africa, using a batch-wise process configuration intended to simulate the revised CSIR-Ti process (Internal document no: CSIR/MSM/LM/IR/2018). All the feed samples were obtained from the same proof-of-concept batch run in which the metallothermic reduction was completed with a 2% stoichiometric excess of $TiCl_4$. The samples were prepared for the leaching experiments by crushing, blending then screening into separate size fractions, according to the methods explained in the following sections.

3.2.1 Sample preparation

After completing the metallothermic reduction run and cooling, a 1500 g sample of the crude product was removed from the reduction retort. The sample was crushed with a forced feed laboratory jaw crusher (BB400, Retsch, Germany) set to a gap of 20 mm under argon gas cover.

The argon gas inlet pipe was connected on the side of the feed hopper but above the crushing chamber to prevent damage to the pipe, and the flow rate was controlled and kept constant at 0.4 l/min with a rotameter (MR3000-3A13, Key Instruments, USA). After crushing, the chips were removed from the bottom collection hopper and then classified into four separate fractions using sieves comprised of the following sizes: 30 mm, 20 mm, 10 mm and 630 µm. The sieves were vibrated in the vertical plane with a sieve shaker (AS 200, Retsch, Germany) for 150 min.

The samples retained on the 10 mm and 630 µm sieves was weighed, blended and split into 20 g samples using the cone and quartering method. Each 20 g sample was transferred to a glass bottle with a screw-on lid and then placed into storage in a secure (bolted and sealed) grade 304 stainless steel vessel flushed with argon before using. It must be noted that the only size fractions considered for the tests were fractions retained on the 10 mm and 630 µm sieves, while the other size fractions were mixed and transferred into 500 ml glass bottles. These bottles were also stored in the stainless steel vessel. Head sample analysis

A composite head sample comprising only the size fractions considered for the test-work was submitted for analysis to determine the total chloride, using the analytical equipment described in Section 3.3.3. The oxygen content was determined by Scrooby's commercial laboratories in Benoni, South Africa, using an Eltra ONH-2000 instrument following the steps and methods stipulated in the ASTM E 1409–97 standard test method for determining oxygen in Ti and Ti-alloys by the inert gas fusion technique. The Li content was determined by inductively coupled plasma optical emission spectrometry (ICP-OES). The result are shown in Table 3.1.

Table 3.1 Initial impurity content in the head sample

Impurity	Chlorides	Oxygen	Li
Mass%	0.3	0.02	3.07

It was concluded that the chemical composition of all the tested samples was the same.

3.2.2 Chemical reagents

The chemical reagents used in all the experiments are listed in Table 3.2.

Table 3.2 List of chemicals used for leaching experiments.

Chemical	Purity	Manufacturer
HCl	32 mass% industrial grade	Protea Chemicals, Wadeville, South Africa
De-ionised water	14 µs conductivity	CSIR-TiCoC pilot plant, Pretoria, South Africa
Argon gas	99.99%	Afrox, Johannesburg, South Africa

*All chemicals were used without any further purification.

3.3 Experimental apparatus and procedure

3.3.1 Apparatus

All leaching experiments were conducted in batch mode, in a 250 ml cylindrical glass vessel fitted with a glass lid equipped with four ports. The central port was fitted with a stirrer shaft, whilst one port was used for pH measurements. The other two ports accommodated an argon gas sparge pipe, a thermocouple inlet and an argon vent pipe connected to the gas trap. Figure 3.1 shows the leaching vessel diagram.

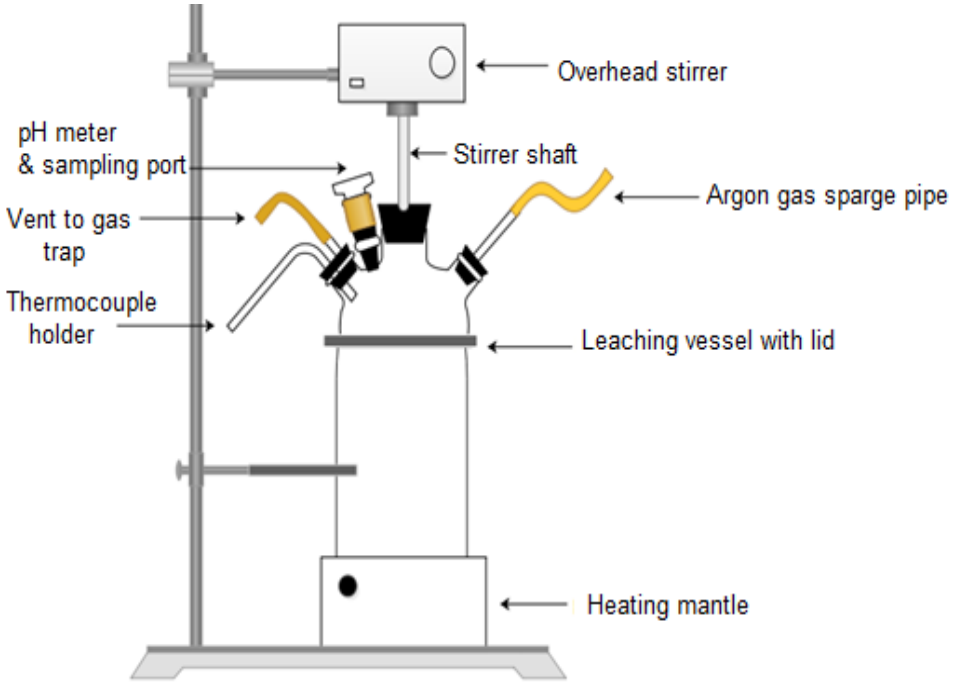

Figure 3.1 Schematic diagram of the leaching vessel and associated equipment.

3.3.2 Leaching procedure

1. Higher temperature (30°–60°C) experiments

The experimental procedure was initiated by transferring 200 ml of the required dilute acid solution concentration (either 1 M or 0.032 M HCl) into the leaching vessel, covering the lid (Figure 3.1) and clamping the lid to maintain it in position, followed by heating the leaching vessel on a heating mantle (Elmulab (Pty) Ltd, South Africa), to achieve the initial temperature of 30°C. The temperature was continuously measured and monitored throughout the experiments with a K-type thermocouple (Hi-Tech Elements, South Africa) submerged in the solution. Temperature readings were recorded onto a multi-channel recorder (RSG30, Endress-Hauser, Switzerland). The solution was agitated with a polytetrafluoroethylene-coated anchor propeller stirrer shaft (Exposed shaft model EX, Fisherbrand™, United Kingdom) fitted on an overhead stirrer (ES, Velp Scientifica, Italy) to maintain the stirring speed at 400 rpm.

The heating mantle was switched off when the solution was at temperature because the leaching reactions are exothermic and the heat generated was expected to increase the leaching solution's temperature (Garmata et al., 1970; Jeppson et al., 1978). As a precautionary step to prevent the temperature from exceeding 60°C at the interparticle interphase, the sample was added slowly while agitating vigorously as per the setpoint (400 rpm) to dissipate the heat into the bulk of the leaching solution. Argon gas was sparged through a pipe with an internal diameter of 25 mm at a flow rate of 0.05 l/min, approximately 10 min before leaching commenced, to ensure a non-oxidative environment. The argon flow was controlled and measured with a rotameter (Key Instruments, MR3000-3A12, USA).

A 20 g solid sample was then added into the leaching vessel. After adding the sample, the leaching solution pH was measured and recorded with a portable pH meter (Russel RL060P, Thermo Scientific, USA), fitted with a glass body pH electrode (Orion 8172 Ross, Thermo Scientific, USA). Thereafter, the pH measurements were recorded periodically at 5, 10, 15, 30 min and 60 min intervals. Upon completing the leaching procedure, the sample was filtered through filter paper (Munktell no. 1, Ahlstrom, Sweden). After filtration, the solid residue was subjected to four cycles of agitated washing in 200 ml of de-ionised water at 30°C to neutralise the acid and dissolve the salt. The de-ionised water temperature was achieved following the process steps described for heating the dilute HCl solution with a heating mantle. The difference between the four washing cycles was the time it took to complete each cycle, with the first cycle conducted for 120 min, the second cycle for 180 min, and the third and fourth cycles lasting 120 min and 60 min, respectively.

The initial and final conductivities of the water in all washing cycles were measured with a portable conductivity meter (EC60 Waterproof EC/TDS/C, Martini Instruments, USA). Upon completing the washing cycles (when the final conductivity was between 14–16 µs), the residue was filtered through the Munktell no.1 filter paper and dried in a vacuum oven (VO400, Memmert, Germany) at 60°C for 6 hours.

The solid residue was not washed with alcohol or acetone to evaporate soluble phases or water despite the advantages associated with this process step with regards to the final product total oxygen content, to mitigate the safety risks posed by the pyrophoric behaviour of fine titanium, as witnessed by other researchers (Bolivar & Friedrich, 2019).

2. Lower temperature (14–30°C) experiments

The experimental procedure conducted in the 14–30°C temperature range was similar to the 30–60°C temperature range, the main difference being that the leaching solution was cooled separately to 14°C in a 1000 ml beaker filled with ice blocks before commencing with the experiments, and then transferred into the leaching vessel. Thereafter, the experiments proceeded with the heating mantle switched off, as explained previously for the higher temperature experiments. The de-ionised water washing process steps were conducted at room temperature.

3. Leaching procedure for determining the degree of chloride removal (acid–leached residue water–washing stages)

To determine the cumulative degree of chloride removal (dissolution) four samples were subjected to Test Nos 1, 3, 5 and 7 HCl leaching conditions. The difference was that the mass and solution volume in Section 3.3.2(1) were changed to 60 g of solid sample and 600 ml; however, the leaching conditions were the same. The cylindrical glass vessel in Section 3.3.1 was changed to a 750 ml vessel to accommodate the new volume. The heating mantle and lid were changed to accommodate the bigger leaching vessel. The fittings setup on the lid were maintained the same as shown in Figure 3.1. Everything else, including the HCl leaching, conditions was as per the procedure specified in Section 3.3.2(1–2) and the variables were in accordance with those in Appendix 1 for the Test Nos selected.

After HCl leaching, the samples were filtered and subjected to three cycles of de-ionised water washing (only leached for a total of 420 min instead of 480 min) as discussed above. The main difference was that after each washing cycle about 10 g of residue sample was removed while the

rest of the sample was subjected to a fresh cycle of washing. The residue sample in each washing cycle was dried at 60°C for 6 hours in the vacuum oven and then subjected to chloride analysis.

The data were used to conduct leaching model calculations and to determine the minimum time required to effectively dissolve the LiCl in order to reduce the chloride content to acceptable level.

3.3.3 Chemical analysis

The dry sample residue was subjected to various analytical techniques to qualify the product's composition and level of purity. The product's oxygen content was determined by combined ON/H analysis (ONH-2000, Eltra, Germany). The total chlorides in titanium were analysed by gravimetry at the South African Nuclear Energy Corporation SOC Limited (NECSA), following the steps and methods stipulated in the ASTM E-120 standard test method for chemical analysis of Ti and Ti-alloys. The samples were further subjected to microstructural examination using scanning electron microscopy (SEM) (JEOL JSM-7001F FEG, Japan), which provided a semi-quantitative analysis of grain compositions. The concentration of lithium in the samples was determined using ICP-OES (Optima 5300DV, Perkin Elmer, USA).

It must be noted that all solution samples were not subjected to more detailed analysis due to financial constraints; as a result, the concentrations of dissolved LiCl and Ti^{3+} ions in the solution could not be determined. Consequently, an opportunity to ascertain some of the observations and assumptions discussed in the literature was precluded.

4 RESULTS AND DISCUSSION

4.1 Experimental design

Experiments conducted in this study are listed in the standard test matrix shown in Table 4.1. The detailed parameters are listed in Appendix 1 and test for repeatability discussed in Appendix 6. The effects of these parameters coded as *A* (initial HCl concentration), *B* (particle size) and *C* (initial temperature) were investigated at low (−1) and high (+1) levels. Eight test combinations and response variables, referred to as *Y*, were yielded. Responses 1 and 2 denote oxygen and chloride assay results in the sample residue mass. [It must be pointed out that all the subsequent results are discussed with respect to the test number combinations listed in Table 4.1.]

Table 4.1 Design matrix of the 2^3 level full factorial design

				Assay Results	
Test No	*A* (M)	*B* (mm)	*C* (°C)	Response 1 (oxygen m%)	Response 2 (chloride m%)
1	0.032 (− 1)	−10 (−1)	14 (−1)	0.10	0.13
2	1.0 (+1)	−10 (−1)	14 (−1)	0.13	0.12
3	0.032 (−1)	+10 (+1)	14 (−1)	0.07	0.22
4	1.0 (+1)	+10 (+1)	14 (−1)	0.09	0.21
5	0.032 (−1)	−10 (−1)	30 (+1)	0.43	0.04
6	1.0 (+1)	−10 (−1)	30 (+1)	0.47	0.09
7	0.032 (− 1)	+10 (+1)	30 (+1)	0.37	0.14
8	1.0 (+1)	+10 (+1)	30 (+1)	0.40	0.10

4.2 Leaching of crude metallothermic reduction product

4.2.1 pH observations

The typical pH behavior observed during the experiments is shown in Figure 4.1(a) and (b), with each group divided according to the initial pH. A comparison of the results indicates that the pH increased rapidly within the first 5 min in all the experiments (Test Nos 1–8). However, considering that pH is a measurement of the hydronium ion (H_3O^+) concentration, these observations were attributed to the high initial consumption of the H_3O^+ ion by the intermediate Li neutralisation reaction step near or on the exposed surface of the particle presented in the solution to form LiOH(aq) by the Li coupled reaction with HCl(aq) to form LiCl(aq) in the final step according to equation [2.17].

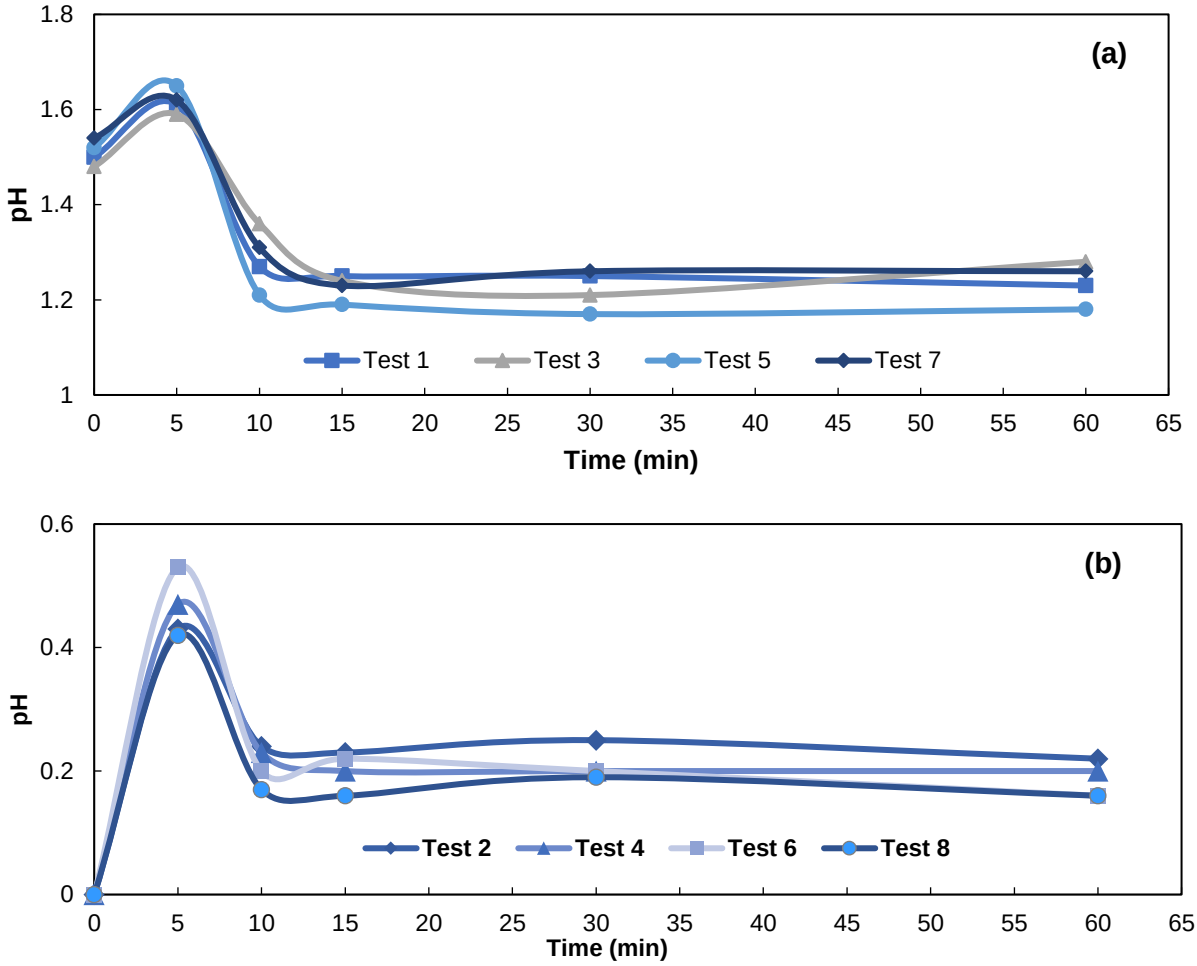

Figure 4.1 Change in pH as a function of time, (a) 0.032 M Initial HCl and (b) 1 M initial HCl.

To quantify this observation, the thermodynamic values (Gibbs free energies for the Li reaction and $TiCl_2$ dissolution reaction in both H_2O and HCl, shown in equations [2.12],[2.16],[2.17] and [2.18]) at the postulated operating temperatures were calculated using HSC Chemistry 7 Software (Chemistry Software, Finland). According to the output data listed in Table 4.2 and Table 4.3, the Gibbs free energy for the Li reaction was more negative than the dissolution reaction of $TiCl_2$ across all the temperature ranges postulated. This suggests that the Li reaction takes precedence over the $TiCl_2$ dissolution reaction. In addition, a comparison of Table 4.2 and Table 4.3 showed that the reaction of Li with HCl takes precedence over its neutralisation reaction in H_2O. This thermodynamic analysis is incorrect, because the Li reaction to form aqueous LiCl is an intermediate chemical reaction that yields LiOH(aq) which ultimately reacts with HCl(aq) to form LiCl(aq). It must be noted that while HSC model software can thermodynamically predict whether a reaction is probable or will proceed as written or not, its limitation is that it cannot predict the kinetics, thus this limitation must be considered when making inferences. The hydrolysis reaction of $TiCl_2$ with H_2O precedes its reaction with HCl, as shown by the more negative Gibbs free energy. By-product compositions in crude titanium sponge and powder—comparison of commercial Hunter/Kroll processes and CSIR-Ti process. Adapted from Garmata et al. (1970). This observation is in good agreement with the assertations by Garmata et al. (1970), who stated that $TiCl_2$(s) in solution is expected to behave like the highly reactive Ti^{2+} ion, even though the reaction is expected to be slow. It further correlates with Figure 2.5, where in TiO_2 is shown to be the most dominant species of titanium in solution at almost all pH ranges.

Table 4.2 Calculated Gibbs free energies of Li and $TiCl_2$ in H_2O

	$2Li\ (s)+ 2H_2O(l) \rightarrow 2LiOH(aq) + H_2(g)$		$TiCl_2(s)+ 2H_2O(l) \rightarrow TiO_2\ (aq/s)+ 2HCl(g) + H_2(g)$	
T (°C)	Δ*H* (kJ)	ΔG (kJ)	Δ*H* (kJ)	Δ*G* (kJ)
10	−397.02	−403.25	−41.53	−135.42
20	−397.77	−403.46	−42.32	−138.72
30	−398.51	−403.64	−43.10	−141.99
40	−399.23	−403.80	−43.88	−145.24
50	−399.94	−403.93	−44.65	−148.47
60	−400.64	−404.05	−45.41	−151.6

Table 4.3 Calculated Gibbs free energies of Li and $TiCl_2$ in HCl solution

	$2Li(s) + 2HCl(l) \rightarrow 2LiCl(aq) + H_2(g)$		$2TiCl_2(s)+ 2HCl(aq) \rightarrow 2TiCl_3(aq)+ H_2(g)$	
T (°C)	ΔH (kJ)	ΔG (kJ)	ΔH (kJ)	ΔG (kJ)
10	−530.92	−576.45	−58.93	−120.49
20	−531.95	−578.04	−60.68	−122.64
30	−532.88	−579.59	−62.27	−124.72
40	−533.77	−581.12	−63.77	−126.76
50	−534.66	−582.62	−65.25	−128.75
60	−535.55	−584.09	−66.71	−130.69

It is also postulated that the H_3O^+ ions were consumed by the hydrogen evolution reaction (HER) at the hydroxide-solution interphase according to secondary equations [4.1] and [4.3] (Kelly, 1982).

$$H^+ + e^- \rightarrow H(ads) \quad [4.1]$$

$$H^+ + H(ads) + e^- \rightarrow H_2(g) \quad [4.2]$$

$$H(ads) + H(ads) \rightarrow H_2(g) \quad [4.3]$$

According to the literature, the HER steps are considered to proceed by three reaction mechanisms, described as ion discharge, electrochemical desorption and recombination according to equations [4.1]–[4.3], respectively electrochemical desorption is believed to be the rate-determining step (Kelly, 1982). Studies on this subject have shown that the $H_2(g)$ evolved is absorbed by titanium sponge or powder, forming an acid-resistant TiH_2 layer on the titanium surface, blanketing the pores and surface (Choi et al., 2019).

After the TiH_2 layer is formed, the diffusion kinetics across the titanium solid matter became the rate-determining step, as detailed elsewhere in the literature (Kelly, 1982; Pourbaix, 1974). This phenomenon was attributed to the peak observed during the initial 5 min interval.

The cumulative acid consumption declined significantly after 5 min, suggesting total consumption of the exposed excess Li metal on the particle surface.

Figure 4.1(a), the pH reached a maximum of less than 1.7, a range where the highly stable $TiOH^{2+}$ was the dominant species, as discussed in Section 2.8.2. Figure 4.1(b) shows that all the pH values reached a maximum of less than 0.7. According to the literature survey, $[Ti(H_2O)_6]^{3+}$ ions are the dominant species of Ti(III) at this pH range. Therefore, the pH decreased due to the resulting H_3O^+ (equation [2.27]), which accounted for the acidity of the solution. These observations were in good agreement with those by Mackenzie and Tompkins (1942), who reported that a decrease in pH values indicates oxidation prevention and hydrolysis, due to subsidiary acidification during the complexation reaction to form $TiCl^{2+}$, as discussed in Section 2.8.2.

The resulting aqueous ions are thermodynamically unstable within the specified pH regions, as demonstrated by the low stability constants in Table 2.4. Hence it is postulated that the ions continued to react by bridging reaction or co-ordination re-arrangement to form stable species and water, which is a product in all the reactions (equation [2.32]). For instance, it is postulated that $[Ti(H_2O)_6]^{3+}$ bridging reaction formed $[Ti(H_2O)_5Cl]^{2+}$ according to equations [2.29]–[2.32], which may be attributed to the stabilisation observed after 10 min.

All the test combinations showed a similar trend even though the initial pH was different, indicating that the first 5 min of the experiments are the most critical. It was also noted that the chloride ion concentration is a major controlling factor. It can be concluded that the power of the complexing ligand and the pH of the media are key factors to stabilising the ions in the solution.

4.2.2 Temperature observations

Examination of the temperature versus time plot shows that the temperature increased sharply within 5 min of adding the crude sample into the leaching vessel during the acid-leaching process. This phenomenon was observed in all the tests, as shown in Figure 4.2(a) and (b). This resulted from the rapid exothermic reaction between the unreacted Li on the exposed surfaces of the crude-Ti with the leaching solution, as discussed in Section 2.8.3. The temperature increases over the 0–5 min interval were experienced despite all the precautionary measures implemented to prevent localised overheating at the reaction-mass–solution interface. Examples of precautionary measures taken were vigorous agitation of the solution, slow addition of the solid sample and the use of a large volume of leaching solution. This suggested a need for simultaneous external cooling.

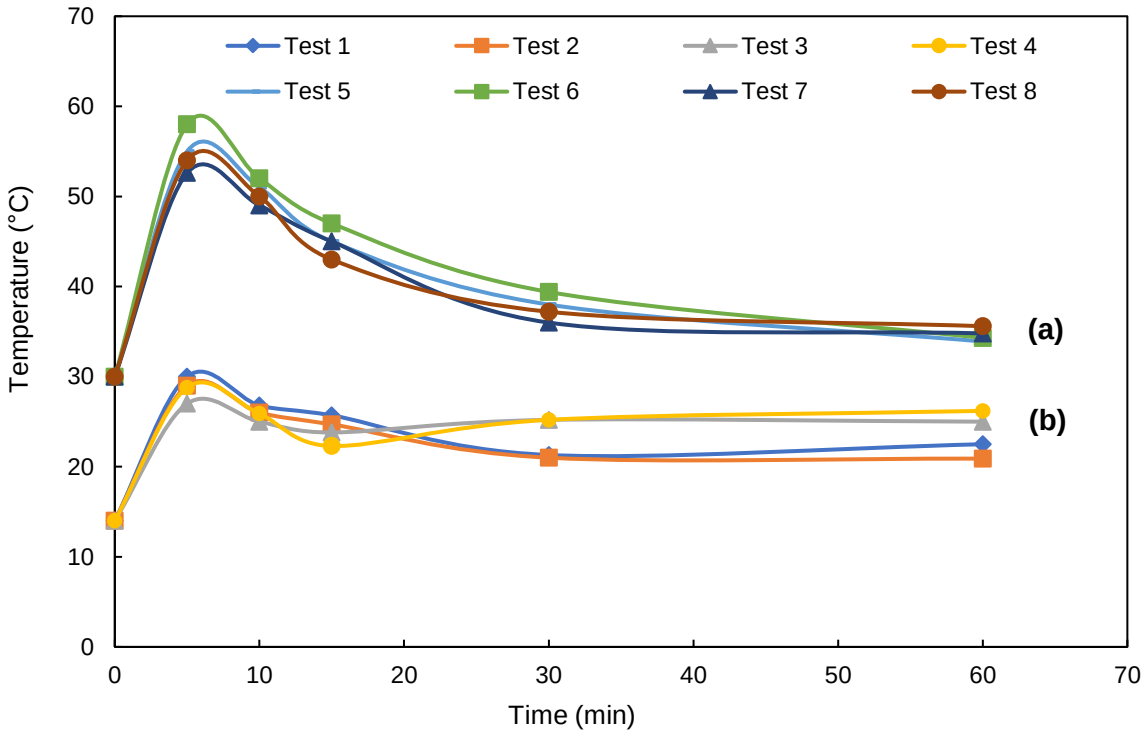

Figure 4.2 Temperature of leaching solution during the leaching process: (a) Initial temperature 30°C and (b) initial temperature 14°C.

The temperature reached a peak and then decreased after 5 min in all the test combinations, which is consistent with the findings discussed in Section 4.2.1. This suggests that after the initial consumption of the excess reagents on the exposed titanium surface, the reaction passed from activation to mass-transfer control due to the formation of the proposed TiH_2 layer on the surface of the titanium particles. At this point, the reaction was dependent on the stirring rate because the latter governs diffusion rate through the TiH_2 layer formed on the surface of the titanium particles. It was further observed that the temperature in Test Nos 1–2 decreased in the final 30 min, due to the smaller particle size of −10 mm. This allowed the exposed by-products to be dissolved and equilibrium to be reached. The solution temperature in Figure 4.2(a) decreased after the initial spike. It continued to do so until the experiments were terminated, suggesting that most exposed and accessible by-products were dissolved by the initial temperature increase, which sped up the solution molecular motion.

The observed temperature response indicates that reactivity is related to the rate at which heat is liberated during chemical combination, rather than the total amount of heat evolved over prolonged periods.

4.3 Final product quality

4.3.1 Oxygen content

The oxygen impurity content of the final product is shown in Figure 4.3. According to the results, the oxygen content is comparable with ASTM standard specifications of 0.18 m% for CP grade 1 to 0.4 m% for CP grade 4. These values were achieved in Test Nos 1–4 and Test Nos 7–8. However, the oxygen levels detected for samples leached in Test Nos 5–6 exceeded the standard specifications. The marked oxygen content increase recorded in Test Nos 5–6 suggests that some $TiCl_2$ occluded in the crude products closed pores might have been dissolved by water to form TiO_2 according to reaction [4.4]:

$$TiCl_2(s) + 2\ H_2O(l) \rightarrow TiO_2(s/aq) + 2\ HCl(aq) + H_2(g) \qquad [4.4]$$

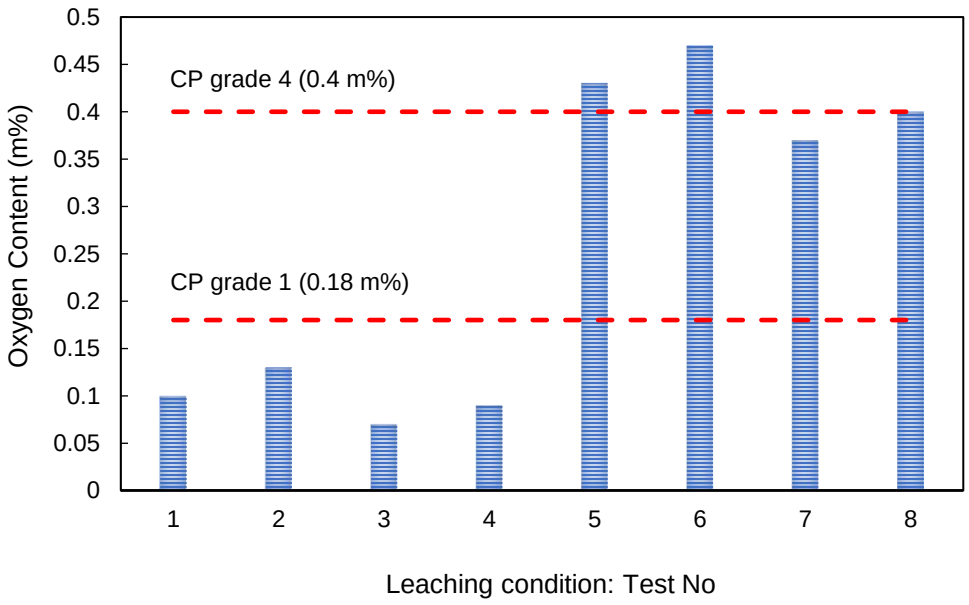

Figure 4.3 Final oxygen contents of CSIR-TI products leached under the experimental conditions listed in Table 4.1.

It was expected that as the salt dissolved during leaching, some fine particles became loose. Some pulverisation might also have occurred through the action of vigorous agitation, resulting in the production of ultra-fines, exposing a higher relative surface area. However, considering the inherent tendency of titanium to form a monolayer of oxide (TiO_2) on its surface in both air and water, the newly developed surface and fines might have oxidised. Consequently, due to the

unfavourable surface-to-volume ratio and increased percentage of surface oxygen relative to the overall mass of particles, this resulted in the increased oxygen content (Van Vuuren et al., 2011). Hansen and Gerdemann (1998), in their studies, demonstrated how the effect of particle size strongly influences the final oxygen content and contamination thereof. They subjected a leached titanium powder for oxygen analysis and, after obtaining an assay of 0.82 m%, screened the sample and separated it into various size fractions ranging from 0.01–4760 µm. When these fractions were re-analysed for oxygen content, they obtained 8.38 m% for the 0.01 µm size fraction and 0.00002 m% for the 4760 µm size fraction.

Some oxygen contamination is also attributed to the water used as a solvent during leaching, which, according to literature, can increase the passivation of oxygen on titanium particles (Kelly, 1982; Liang et al., 2020). Garmata et al. (1970) reported the degree of oxidation for leach water temperatures between 30°C and 100°C to be between 0.0025% and 0.1%. Hence, it may be assumed that the increase was related to this phenomenon because the samples were exposed to temperature increases during acid leaching due to the exothermic nature of the reactions. The system temperature plots indicated that some oxygen contamination might have emanated from precipitation of the hydrolysis products due to localised overheating on particle–particle surface contact during leaching.

The initial oxygen content of 0.02 m% compared with the leached sample oxygen contents (Figure 4.3) indicates that the final oxygen content obtained in all the tests increased as postulated. However, the increment could be classed as insignificant in Test Nos 1–4, because the final product content was below 0.18 m% for CP grade 1. Hence, the result indicates that, while oxidation by water is inherent to acid leaching, hydrolysis of by-products and contamination thereof can be minimised when operating parameters such as the solution acidity and leaching temperature are controlled effectively.

4.3.2 Total chloride content

The chlorine in titanium sponge and powder exists as total residual chlorides, which collectively correspond with the chlorine ions in LiCl, $TiCl_2$, $Ti(OH)Cl_2$ and Ti(OH)Cl. Total chloride must be reduced to between 0.12–0.15 m% or lower for titanium sponge (Nechaev & Polezhaev, 2016; Yan et al., 2015; Yu & Jones, 2013).

Examination of the data in Figure 4.4 revealed that the total residual chloride content in the purified product decreased with an increase in temperature and particle size. It was apparent that residual chlorides were significantly lower in the samples washed with de-ionised water at an average temperature of 30°C (Test Nos 5–8), unlike those washed at 14°C (Test Nos 3–4).

However, the chloride content in sample Test Nos 1–2 was similar to Test No 7 despite the samples being leached at a low temperature. The anomaly was attributed to the smaller particle size of −10 mm relative to the +10 mm in Test No 7, which presented a large surface area per unit mass, resulting in an increased extent of leaching. Test No 8 also presented lower chloride content despite its +10 mm size fraction due to the high leaching temperature.

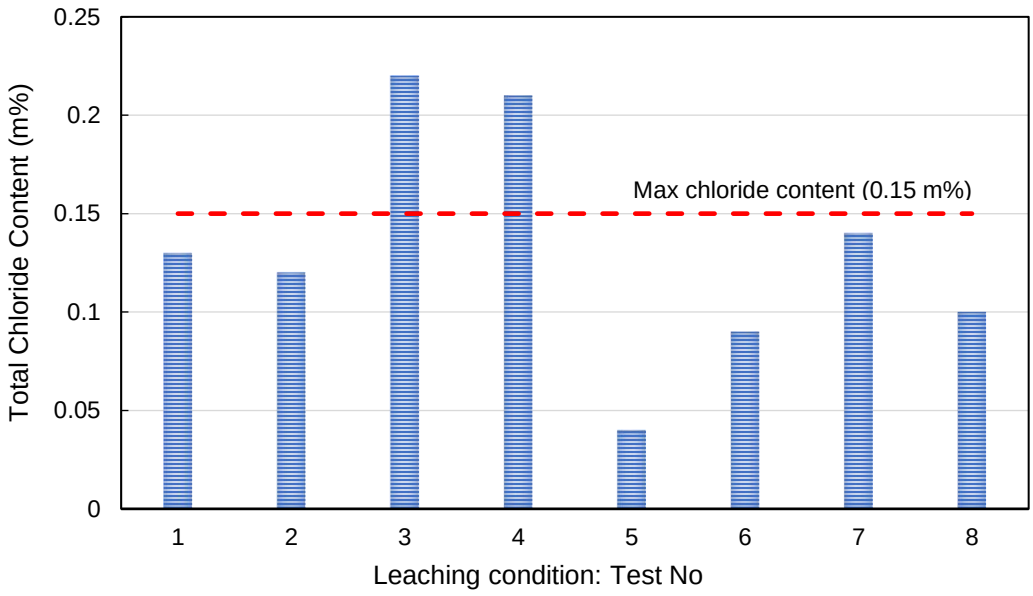

Figure 4.4 Total residual chloride content in the final product leached under experimental conditions of Test Nos 1–8 listed in Table 4.1.

The degree of chloride removal ($ń_e$) was calculated from the ratio of concentrations according to equation [4.5] (Nechaev & Polezhaev, 2016):

$$ń_e = 1 - {}^{C}/_{C0} \qquad [4.5]$$

where C_0 and C are initial and final total chloride contents in titanium powder or sponge, respectively. The initial head sample chloride concentration of 0.30 m% was used for all

calculations. The orders of degrees of chloride removal arranged from Test Nos 1–8 are shown in Table 4.4.

According to the results, a combination of small particle size (−10 mm), high exothermic temperature and de-ionised water washing temperature of 30°C resulted in enhanced LiCl dissolution rates as evidenced by the $\acute{\eta}_e$ of Test Nos 5-8. This suggests that the high temperature led to improved collision probability between the particle and leaching reagent. This concept is explained by the Arrhenius equation, $k = k_0 e^{-E/RT}$, in which the reaction-rate constant k is exponentially dependent on temperature (Yang, 2019). However, the $\acute{\eta}_e$ for Test Nos 1-2 was also higher despite the low leaching temperature of 14°C. The incongruity was ascribed to a decrease in particle size. This is attributed to the specific surface area of the particle, which increased with a decrease in particle size. Consequently, the small particle size facilitated dissolution by maximising the collision probability of the leaching agent and the particle as well as diffusion of the agent into the pores of the particle. Based on these observations, it was clear that particle size and temperature exhibit a considerable influence on LiCl dissolution as evidenced by Test No 5.

Table 4.4 Degrees of chloride removal

Test No	Particle size (mm)	Leaching Temp (°C)	C_0 (m%)	C (m%)	$\acute{\eta}_e$
1	−10	14	0.30	0.13	0.57
2	−10	14	0.30	0.12	0.60
3	+10	14	0.30	0.22	0.27
4	+10	14	0.30	0.21	0.30
5	−10	30	0.30	0.04	0.87
6	−10	30	0.30	0.09	0.70
7	+10	30	0.30	0.14	0.53
8	+10	30	0.30	0.10	0.67

In addition to temperature and particle size, another equally key factor that determines the complete removal of the residual chlorides is the morphology of the titanium sponge or powder. To elucidate this, the purified product or powder was characterised by SEM.

The SEM micrograph study in Figure 4.5(a) and (b) showed that the CSIR product had an irregular coral-like porous structure akin to a sponge or agglomerates, as pointed out by the labelled

numbers and arrows. The pore distribution appeared flat, non-uniform and microporous, as illustrated by the magnified micrograph of the pores in Figure 4.5(c).

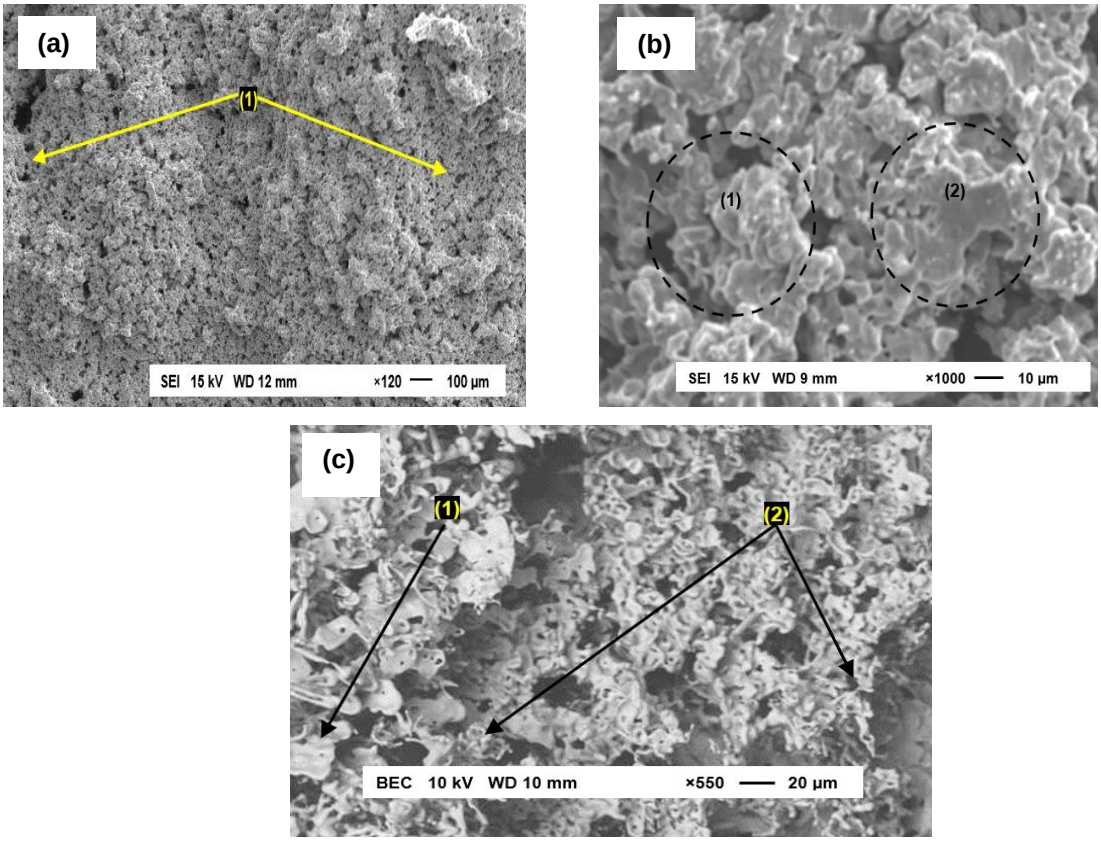

Figure 4.5 SEM micrographs of the product after leaching in Test No 6 at (a) low magnification, (b) higher magnification and (c) magnified pore micrograph.

The high magnification also revealed that during crushing to achieve the −10 mm size fraction in addition to propagating cracks and opening isolated pores, some particles were also flattened, as seen in point 1 and 2 of Figure 4.6(a). The formation of sintered and flattened agglomerates with semi-closed voids or closed pores impedes LiCl removal during leaching. Sintered grains and dendritic particulates were also detected, as shown in Figure 4.6(b). The sintering is attributed to prolonged contact between titanium crystals forming in the molten salt and overheating on the surface of the metal during the metallothermic reduction. Sintering resulted in salt entrapment in the closed pores of the powder. The disadvantage of this process phenomenon is that the salt entrapped in this form cannot be removed completely, even if the residence time is increased.

The entrapment of salt in the microstructure is also a pertinent problem experienced in the HDH and Armstrong process powders (Peter et al., 2012)

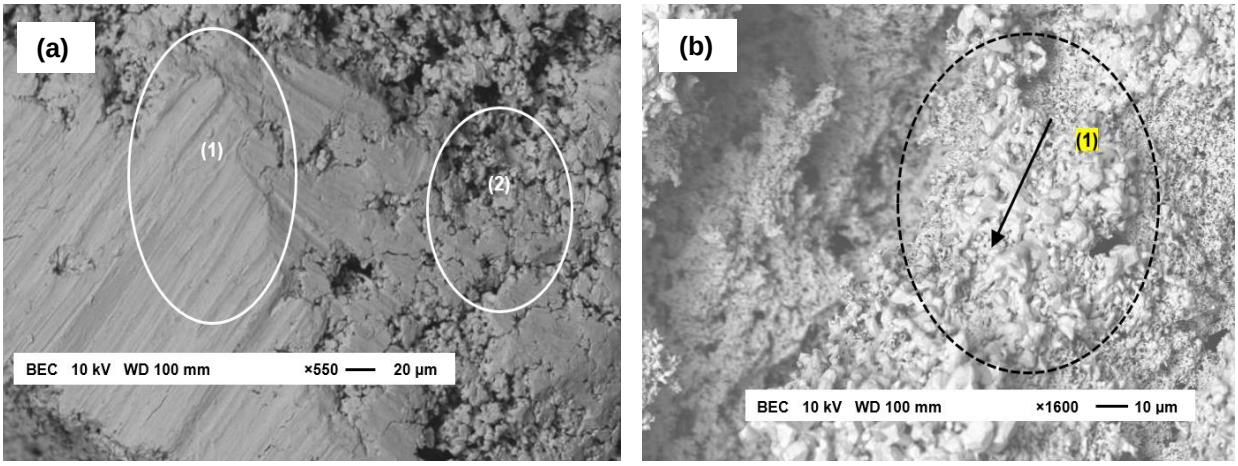

Figure 4.6 Magnified micrograph of the purified residue in Test No 6 showing (a) the effects of crushing on the product morphology or structure and (b) evidence of sintering.

A micrograph of a mounted sample that had been leached following Test No 4 conditions, showed a bright intensity which represents the presence of Li and some hydrated LiCl spheres as illustrated in Figure 4.7. This identification was crucial in that it provided strong evidence that when LiCl adsorbs moisture in the atmosphere during storage or processing, it forms hydrates. Given that LiCl is extremely soluble in water, for instance, the solubility of monohydrate $LiCl.H_2O$ is about 20 $mol.kg^{-1}$ in pure H_2O at 25°C, it may react with titanium powder and metallic impurities in the powder leading to more contamination (Monnin et al., 2002; Nechaev & Polezhaev, 2016).

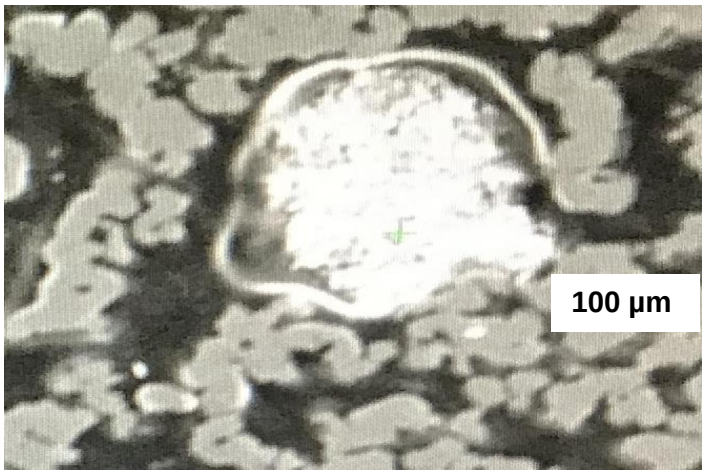

Figure 4.7 Mounted cross-sectional micrograph of the leached powder in Test No. 4.

It can be concluded that the chloride content in Test Nos 1–2 and 5–8 met the general maximum specifications. The chloride content level of 0.04 m% obtained in Test No 5 met the maximum specification range of 0.08 m% found in HDH powder (Yan et al., 2015). In addition, it also met the highly recommended value of 0.05 m%, but was significantly greater than the ideal 0.01 m% concentration for premium metal powders (Van Vuuren et al., 2011; Withers et al., 2013). Hence, considering the low final pH values obtained in the experiments, as shown in Figure 4.1, the possibility of forming oxychlorides was reasonably low. Thus, it is postulated that the chloride impurities emanated from LiCl trapped physically by sintering or mechanically by crushing.

4.3.3 Effect of particle size

To summarise the effect of particle size on the CSIR leaching system, the chloride content is considered to facilitate the discussion. A good correlation of the residual chloride results entails considering the effect of particle size because the interfacial area between the solid:liquid interface increases with a decrease in particle size, a phenomenon proven by the degree of chloride removal in Table 4.4 and Figure 4.4, wherein the lowest chloride content was obtained in all the −10 mm size fractions. The small particle size resulted in a reduced distance within the porous structure of the solid through which the solute had to diffuse. As a result of this phenomenon, the degree of chloride removal in Test Nos 1–2 in Table 4.4 was high despite the samples being leached and rinsed at 14°C. It was also observed that a combination of −10 mm size fraction and 30°C washing temperature resulted in the highest degree of removal obtained in Test No 5–6. This is attributed to the increased diffusion coefficient as a result of the increased temperature (Richardson et al., 2002).

It was observed that the increase in particle size, while having a negative effect on complete chloride removal, resulted in a low oxygen content, as discussed in Section 4.3.1.

The effect of particle size was also observed in the change of temperature (Figure 4.1(a) and (b)), wherein it was noted that all the test combinations showed a similar trend even though the initial leaching temperatures were different. This indicated that the first 5 min of the experiments are the most critical as the hydrometallurgical treatment of the reaction mass depends on the specific surface area of the powder or sponge. It was observed that after the initial 5 min the +10 mm size fraction temperature reached a peak followed by a dead-time zone wherein the temperature was steadily decreasing. This was also observed in the −10 mm size fraction, where the temperature decrease persisted until the acid leaching cycle was terminated. This indicated that the small size

fraction increased contact area, thus accelerating the reaction between impurities and leaching agent. In addition, the cracks propagated by the crushing the particles to achieve the −10 mm size fraction led to increased stress and energy in the lattice, which reduced the reaction activation energy. It was observed that with the +10 mm size fraction the residence time and agitation resulted in the dissolution of by-products, thus the increase in temperature towards the termination of the acid leaching cycle. This observation was more prominent in Test Nos 4 and 8.

Based on this, it was concluded that the effectiveness of leaching and complete removal of dissolved impurities from the sponge or powder is dependent on leaching kinetics. However, kinetics is a factor of agitation, chemical reaction, temperature, particle size and morphology.

4.4 Factorial design analysis

4.4.1 Design of experiments

The relative effects of initial HCl concentration (*A*), particle size (*B*) and temperature (*C*), and their associated interactions on the oxygen and chloride content in the purified product were calculated using equations [7.1]–[7.7] in Appendix 2. The results are listed in Table 4.5. The calculation was based on the assumption that the estimates of the factors are deviations of the mean negative settings from the mean positive settings of the individual factors on test parameters (Montgomery, 2017; Sarswat, 2010).

Table 4.5 Factorial design calculation of the individual factors and their interaction using the oxygen and chloride contents in the final product as the response variables

				Interaction of variables			
	A (HCl)	*B* (P/S)	*C* (Temp)	*AB*	*AC*	*BC*	*ABC*
Oxygen	0.015	−0.025	0.160	−0.003	0.003	−0.008	6*E−18
Chlorine	−0.0013	0.0363	−0.039	−0.011	0.004	−0.009	−0.011

It must be noted that for the interpretation of the data in Table 4.5, the objectives of the experimental work had to be considered because the general factorial equations are limited by the coded factors (−1 for minima and +1 for maxima), and thus, cannot clearly distinguish the actual effect or confirm the magnitude of the significance of the tested factors as indicated by the interaction values. However, this limitation can be addressed by using the factorial DOE in conjunction with a statistical analysis package.

The data in Table 4.5 indicate that an increase in the initial HCl concentration (*A*) from low to high level had a positive effect of 0.015 on the oxygen results and a slightly negative effect of −0.0013 on the chloride content removal; thus, when the HCl concentration was high, the rate of chloride removal was low. Theoretically this conclusion is logical because the presence of HCl results in a chlorine common-ion effect, which is supposed to slow down the dissolution kinetics of LiCl. However, it must be noted that this phenomenon was only observed in Test No 5, because in actual fact dissolution is a factor of various other variables as per the conclusion in Section 4.3.3. Similarly, the increase in particle size (*B*) from low to high had a –0.025 decrease on the oxygen content; thus, when the particle size was high, the oxygen content is low. Furthermore, when the particle size was high the chloride content is expected to be high. The increase in temperature (*C*) from low to high had a very substantial (average of 0.16) effect on the increase of oxygen content and –0.0388 decrease on the chloride content in the purified product; consequently, when the temperature is high, the chloride content is low. The effect of the interaction of factors (*ABC*), irrespective of the combination, was found to be negligible on the oxygen content. However, it had a slightly negative effect on the chloride dissolution due to the increased particle size, compounded by low temperature resulting in slow dissolution kinetics.

Of the relative individual and interactions evaluated, it was established that temperature (*C*) had the highest value and consequently had the largest effect on the oxygen content and chloride content in the purified product.

4.4.2 Analysis of factorial design of leaching experiments

A screening test to identify the individual factors and mutual interactions with a significant effect on the chlorides and oxygen content in the final product (Figure 4.3 and Figure 4.4) was conducted using the Expert Design 12.0 statistical program (Stat-Ease, Inc., 2020). The accuracy of the fitted model was determined by the coefficient of determination (R^2) output from the software. Analysis of variance (ANOVA) was used to analyse the statistical significance of the factors and their interaction. According to the model, for the factor or interaction of effects to be deemed statistically significant, the *P*-value obtained has to be < 0.05 at a confidence interval of 95% (Montgomery, 2017). A small *P*-value means that not all the main effects and interactions are zero at a 5% significance level (Sarswat, 2010). The *F*-value of overall significance is also used to establish the extent to which the mean in the experimental conditions differs more than would be expected (Sarswat, 2010). Therefore, if large, it means the effect of the variable or interaction is significant and it is not due to noise.

The Expert Design 12.0 statistical software uses graphical tools on half-normal plots to split the tested effects (factors investigated) into two groups of significant and insignificant effects based on the response variable. For example, Figure 4.8(a) shows that temperature, particle size and initial HCl concentration are the factors with the most significant effect on oxygen as they are the only factors that did not fit on the normal distribution line. Factors with significant effect on residual chlorides content were particle size and temperature, as shown in Figure 4.8(b). Hence this principle was used to discriminate between some factors and interactions in the analysis of the factorial design with ANOVA in the subsequent sections.

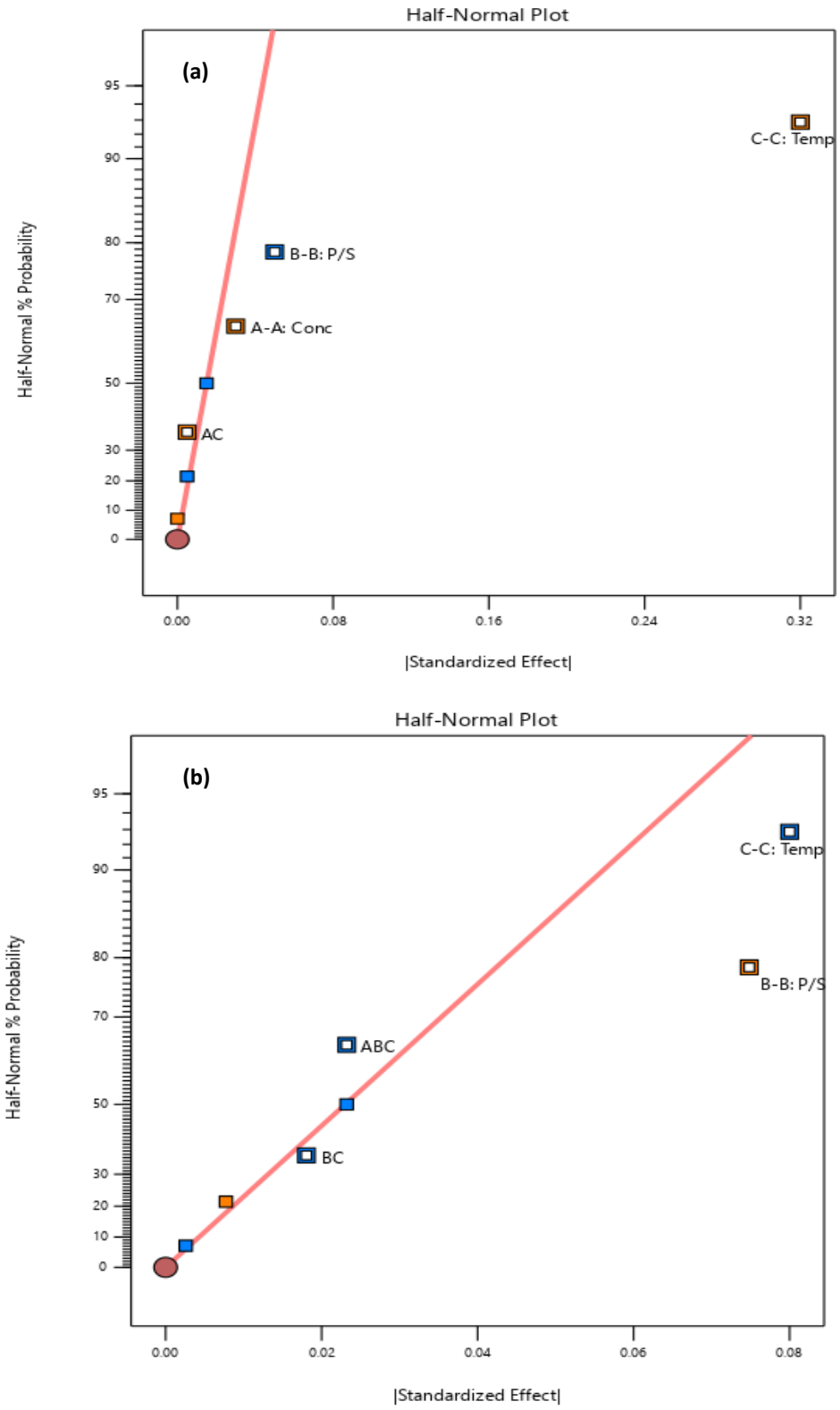

Figure 4.8 Standardised half normal percentage probability for the leaching tests (a) oxygen content and (b) total residual chlorides content.

4.4.3 Analysis of factorial design for oxygen content

The *P*-values examination in Table 4.6 shows that the experimental parameters with a significant effect at the 0.05 validity boundary level on the oxygen content in the final product were particle size (*P/S*), temperature, and concentration. The model *P*-value of 0.0003 implied that the effects of temperature, initial HCl concentration and particle size on the final oxygen content were significant.

Table 4.6 Analysis of variance for the concentration of oxygen in the leached product

Source	Sum of squares	Degree of freedom	Mean square	*F*-value	*P*-value
Model	0.2116	4	0.0529	317.48	0.0003
A: Conc	0.0018	1	0.0018	10.80	0.0462
B: P/S	0.0050	1	0.005	30.00	0.0120
C: Temp	0.2048	1	0.2048	1228.80	<0.0001
AC	0.0000	1	0.0005	0.3000	0.0622

*R-sq = 99.76%, R-sq (pred) = 98.32% and R-sq (adj) = 99.45%.

According to the inferences made in the literature survey of this study, acid concentration was the factor with the most significant effect on the final oxygen content in the purified product. However, according to the *F*-value, the effect of concentration was not the most significant of all the three factors. This inconsistency is a consequence of the assumption that insoluble compounds such as LiOH, TiO_2, $Ti(OH)Cl_2$ and Ti(OH)Cl are the sources of oxygen impurity when the acid concentration is insufficient to prevent hydrolysis and consequently precipitation (Choi et al., 2019; Kelly, 1963; Liang et al., 2020). This assumption is dependent on the initial $TiCl_2$ and Li content in the crude titanium product, which consequently determined the Ti^{3+} and Li^{+} ion concentrations. Precipitation only occurs when the activities of the ions exceeds the thermodynamic equilibrium constant (K_T) (Choi et al., 2019; Free, 2013). Considering the low maximum pH levels observed in Figure 4.1(a) and (b), it may be concluded that the discrepancy in the model is in good agreement with inferences made in the potentiometric titration studies by Ashton (1977), who

showed that at a base to $Ti(H_2O)_6^{3+}$ ionic species ratio of 1:1, only primary hydrolysis takes place to form soluble species.

The startling effect of temperature on the oxygen concentration observed in the DOE model was in reasonable agreement with the prediction that the rate of oxidation of titanium in water increases with an increase in temperature. The high *F*-value is justified because an increase in temperature influences precipitation; therefore, for the CSIR system, ineffective agitation may lead to localised overheating.

The DOE model could not detect the significance of the interaction between temperature and pH, even though, in actual practice, the two factors cannot be considered in isolation, as illustrated by the Van't Hoff isotherm for chemical reactions. The equation relates the Gibbs free energy of reaction, temperature and the equilibrium constant according to equation [4.6] (Free, 2013):

$$\Delta G^{\circ} = -2.303\, RT \log k \qquad [4.6]$$

where R is the ideal constant (8.314 J mol^{-1} K^{-1}) and T is the temperature as the function of log k the equilibrium constant.

According to this equation, an increase in temperature decreases the equilibrium constant and, consequently, a shrinkage in the Ti(III) ion stability region. Therefore, when considering that the hydrolysis of Ti(III) ions occurs at pH values around 0.6, it may be concluded that some Ti(III) might have hydrolysed due to this phenomenon on some surfaces due to localised overheating on some particle leading to the formation of either TiO_2 or $Ti(OH)_3$. However, given that the *P*-value of 0.062 obtained was much closer to the recommend *P*-value despite being high, it is concluded that the effect of the interaction must have been statistically significant and consequently influenced the final oxygen content in the product.

Since the confidence intervals for the factors investigated in this study was above 95%, it is concluded they each had an independent significant influence on the oxygen content in the final product.

4.4.4 Analysis of factorial design for chloride content

The ANOVA results in Table 4.7 show that the individual effects of both temperature and particle size on the total residual chloride removal were statistically significant at the 0.05 boundary level. However, their interaction was not statistically significant, as evidenced by the large *P*-value of 0.3459 > 0.05. This proved that mass transfer through a particle is not just a factor of the size but also the morphology, which determines the path through which mass transfer must occur. The statistical analysis also indicated that the effect of temperature was more significant than all factors and interactions. This finding correlates with the deductions made in Section 4.3.2.

Table 4.7 Analysis of variance for the concentration of total residual chlorides

Source	Sum of squares	df	Mean square	*F*-value	*P*-value
Model	0.0231	3	0.0077	14.35	0.0132
B: P/S	0.0105	1	0.0105	19.56	0.0115
C: Temp	0.0120	1	0.0120	22.35	0.0091
BC	0.0006	1	0.0006	1.14	0.3459

**ABC* was not included in the model due to the significant error introduced due to not considering factor A because it lies on the normal distribution line.

**R-sq = 90%, R-sq (pred) = 70% and R-sq (adj) = 90%.

4.4.5 Discussion of the statistical analysis model fitting

A model is regarded as having well-fitted data or accurately describing the relationship between the variables and the response variables when the coefficient of determination (R^2) and adjusted R^2 for the degrees of freedom (R^2_{adj}) are closer to or equal to 1 (Montgomery, 2017). The R^2 and R^2 (R_{adj}) for the oxygen model (Table 4.6) were 99.8% and 99%, while the R^2 (predicted) was 98%. The R^2, R^2 (R_{adj}) and R^2 (predicted) values for the chloride model (Table 4.7) were 90%, 90% and 70%, respectively. The R^2 (predicted) for the chloride model was low, indicating that the model is unlikely to be a good predictor of the variability should the data be changed (Montgomery, 2017). It was revealed that the experimental data for the oxygen content fitted the predicted value in the model well, while that of the chloride content did not, for the reasons discussed above.

The R^2 and R^2 (R_{adj}) values for both response models in the present study correlates with the experimental data and observations. Hence the developed model can be used to guide the developmental stages.

4.4.6 Simple statistical optimisation of the model

The results were optimised to determine the potential improvement and the optimal leaching parameters that would yield a product that conforms to both chloride and oxygen concentration specifications. This was achieved by re-calculating the models. In the re-calculation, the maximum temperature was maintained at (30°C) while varying the initial concentration and particle size. The temperature of 30°C was selected because it yielded the best chloride content in the product as per Table 4.1. The decision to hold temperature constant was based on the statistical analysis model, which showed that temperature was the factor with the most effect on the response variable (oxygen and chloride content in the final product). A three-dimensional (3D) response plot showing the optimal conditions for this model was constructed, as shown in Figure 4.9(a) and (b). However, on account of the model only containing the main effects and no interaction, the fitted response surface is a plane, a characteristic of a first-order model (Montgomery, 2017).

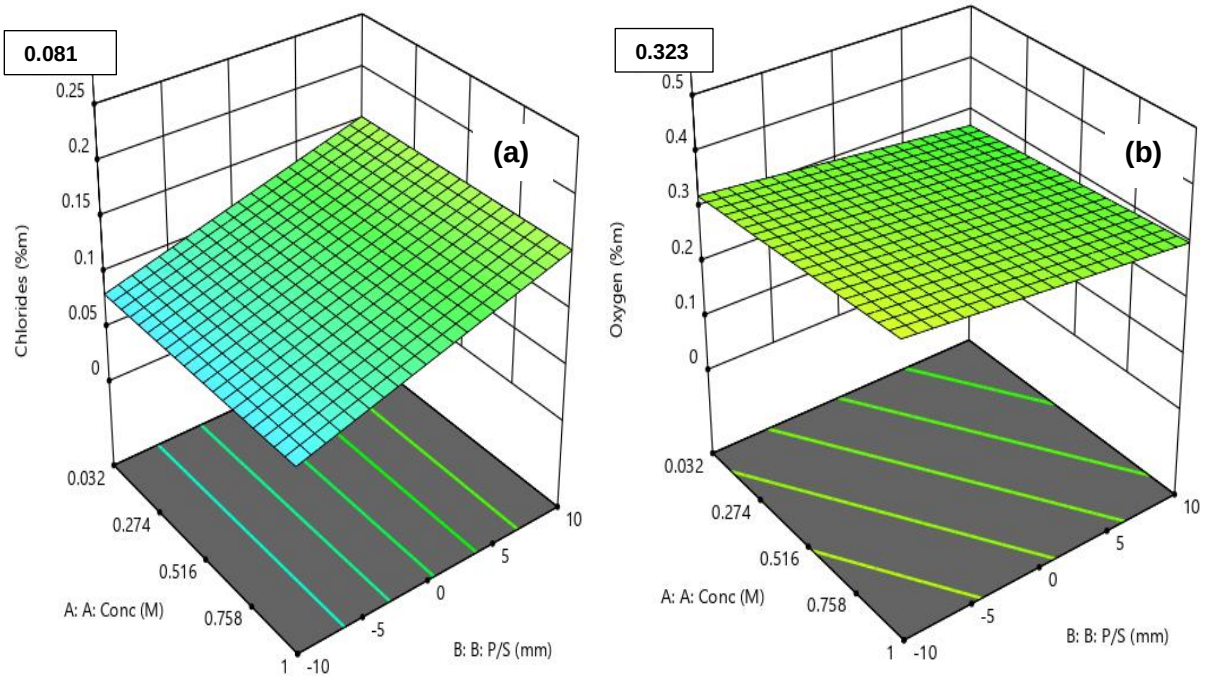

Figure 4.9 Response surface plot for (a) total residual chloride and optimal oxygen (b) vs. varied factor parameters, based on the outputs of factorial design.

According to the plot, the total chloride content of 0.08 m% and an oxygen content of 0.32 m% can be obtained when the product particle size is reduced to −10 mm and leached in dilute HCl with an initial concentration of 0.032 M at 30°C.

4.5 Kinetic analysis of the chloride removal (acid–leached residue water–washing stages)

Most leaching processes follow the kinetic models for heterogeneous solid–liquid reactions known as shrinking-core models, as discussed elsewhere in the literature (Free, 2013; Yang, 2019). According to the shrinking-core model, the overall kinetics of a reaction is controlled by either chemical reaction at the surface or diffusion through the solid product layer (Habashi, 1999). The model also assumes a spherical particle shape (Yang, 2019).

For a surface chemical reaction-controlled process, the kinetics are described by equation [4.7]:

$$1 - (1 - x)^{\frac{1}{3}} = K_r t \qquad [4.7]$$

where: x is the cumulative chloride fraction removed (assumed to be a direct consequence of the degree of dissolution), determined using equation [4.5], t = leaching time and K_r = is the first-order rate constant (m/s).

An internal diffusion-controlled model where diffusion through a reacted layer of increasing thickness is the main controlling factor is described by equation [4.8]:

$$1 + 2(1 - x) - 3(1 - x)^{\frac{2}{3}} = K_d t \qquad [4.8]$$

where x is the cumulative chloride fraction removed and t is time. K_d is the dimensionless solid product layer diffusion rate constant.

The cumulative chloride degree of removal data for acid–leached residue after the water–washing stages were fitted to leaching models to determine the rate–controlling step. This was achieved by subjecting four of the test combinations to de-ionised water washing steps at various time intervals after acid leaching and then analysing for total chloride content, as displayed in Table 4.8. The assumption made was that when leached under the same test combinations, the final chloride analysis at time 480 min would be the same as those obtained in Figure 4.4 because the LiCl washing was terminated at 420 min; thus, if the washing cycle was extended by 60 min, the final chloride contents would be similar to those obtained at 480 min. Thus, the tested samples

were only washed until time interval 420 min. A cumulative degree of chloride removal was calculated following the method discussed in Section 4.3.2 and equation [4.5]. The resulting values are displayed in Figure 4.10.

Table 4.8 Chloride content in water-washed samples at various time intervals

Leaching period (min)	Chloride content (m%)			
	Run 1	Run 3	Run 5	Run 7
0	0.3	0.3	0.3	0.3
120	0.26	0.27	0.23	0.27
300	0.19	0.25	0.14	0.2
420	0.15	0.23	0.07	0.16
480	0.13	0.22	0.04	0.14

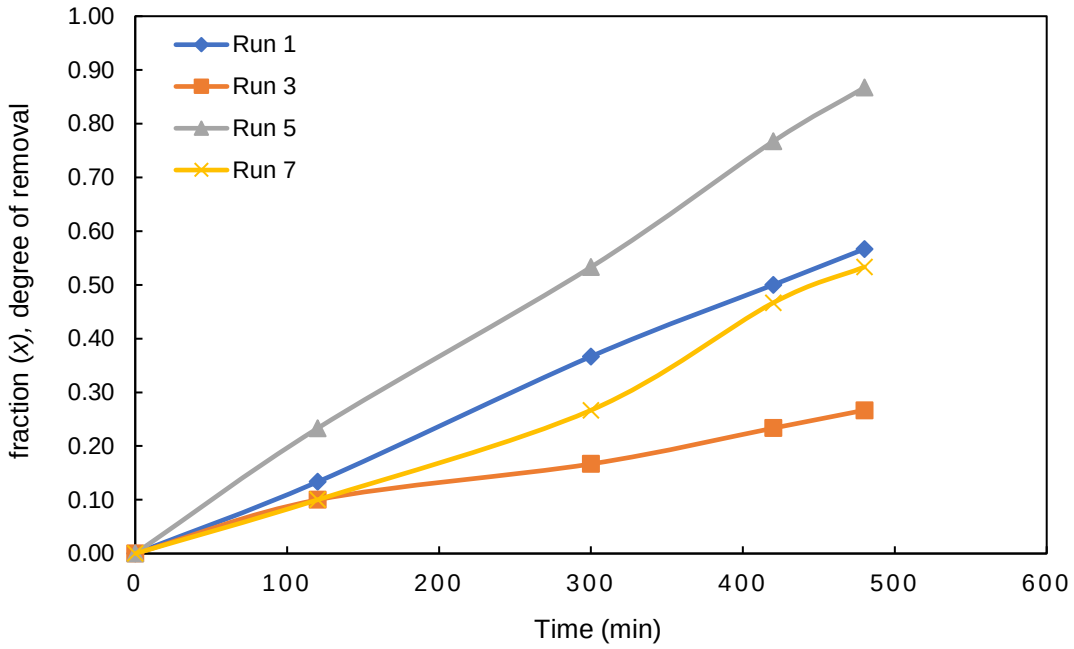

Figure 4.10 Cumulative degree of removal of total chlorides at various time intervals and test combinations.

The fits of data for both models are presented in Figure 4.11 and Figure 4.12.

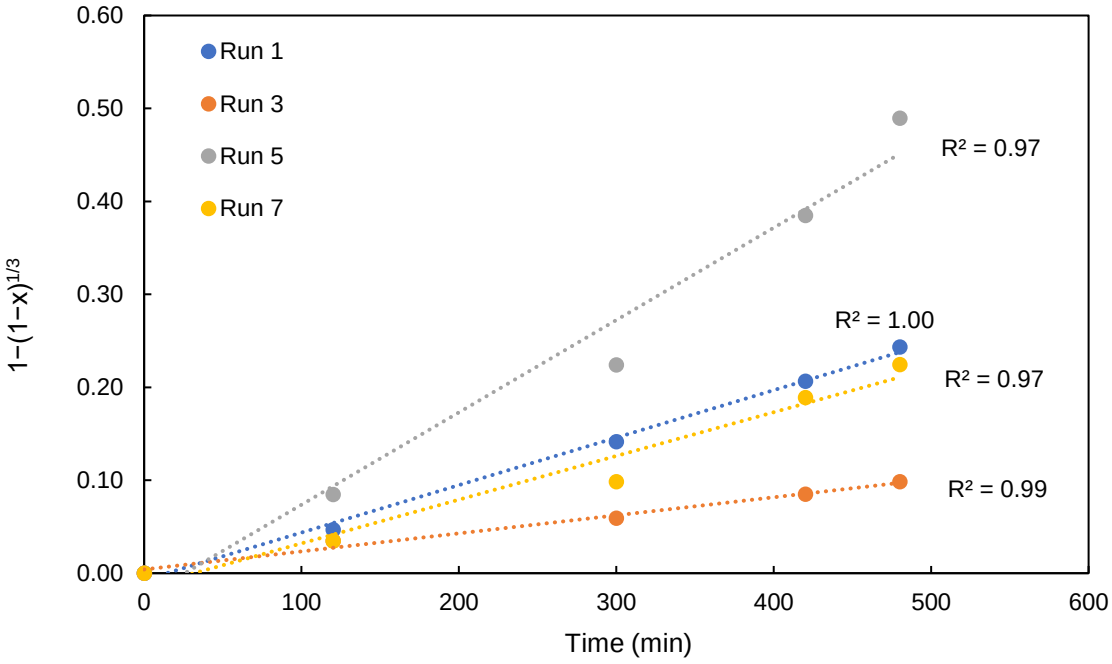

Figure 4.11 Plots of $1 - (1 - x)^{1/3}$ versus time under different acid-wash conditions.

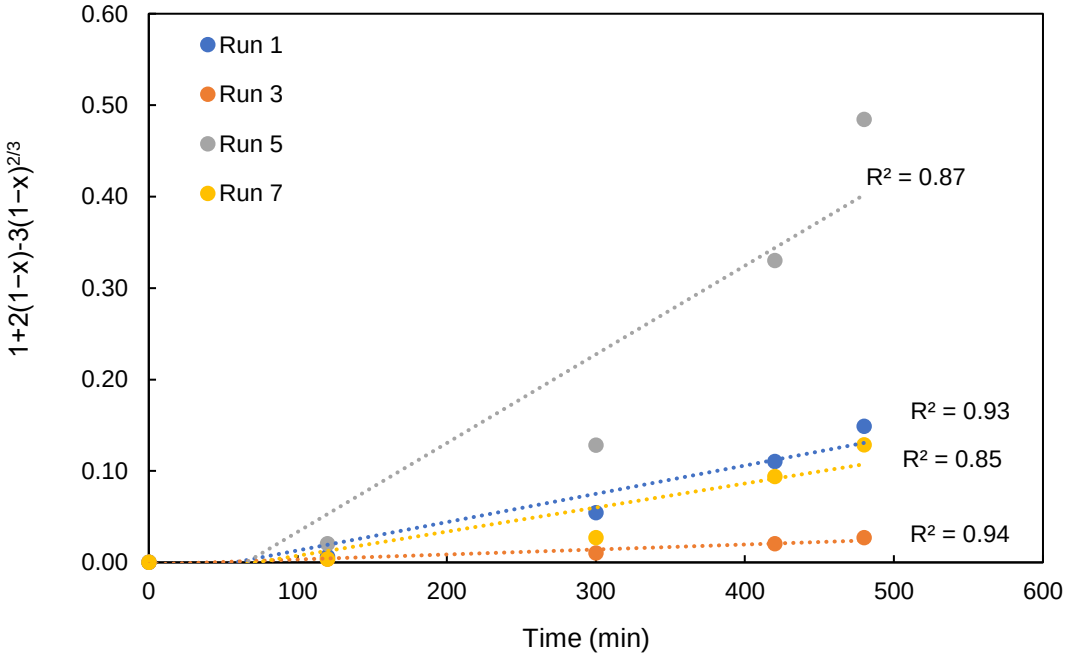

Figure 4.12 Plots of $1 + 2(1 - x) - 3(1 - x)^{2/3}$ versus time under different acid-wash conditions.

By comparing the regression coefficient values correlating the rate to the data in both Figure 4.11 and Figure 4.12, it was established that Figure 4.11 gave the best linear relation for all leaching test combinations. Consequently, it may be circumstantially concluded that the CSIR leaching system is surface chemical-reaction controlled. This implies that the TiH_2 product layer formed on the titanium surface does not inhibit the reaction to any appreciable extent, as had initially been thought. Thus, as asserted by Habashi (1999), these systems are characterised by a high dependence on temperature. This conclusion is in good agreement with the statistical analysis, wherein it was established that temperature was the factor with the most significant effect on the chloride results. Considering that the kinetic analysis was conducted for the water–washing stages, it must be noted that this kinetic model might not be comprehensive. This is because most of the factors with effect on the kinetics and models thereof (such as concentration, HER evolution, TiO_2 surface layer formation, diffusion, heat evolution etc.) occur during acid leaching and are only experienced to a limited extent during water washing.

5 CONCLUSIONS AND RECOMMENDATIONS

The results from this study have demonstrated that acid leaching can be used to purify crude titanium produced using the CSIR-Ti process. However, based on the SEM micrographs, the hygroscopic nature of the residual LiCl is a concern, especially when considering storage and processes requirements downstream.

The statistical analysis of the factorial design of experiments to establish the effects of initial HCl concentration, temperature and particle size on crude-Ti leaching indicated that, of the three factors investigated, temperature was the factor with the most statistical significance on the oxygen and chloride contents in the purified product. The DOE model optimisation results indicated that the best cut-off point for both oxygen and chloride will be achieved at a temperature of 30°C, a temperature at which the chloride content of 0.08 m% and oxygen content of 0.32 m% will be achieved. However, this will only meet CP grade 4 standard specifications. For the leaching procedure to be technically feasible, control measures to dissipate the effects of localised overheating emanating from the exothermic heat evolved by the neutralisation reaction of Li will have to be in place.

The pH trends showed that the leaching mechanism of the by-products in the crude product followed primary hydrolysis behaviour. This is a region in which Ti(III) remains in solution as an ionic species, because the concentration of the OH^- ion was insufficient to effect secondary hydrolysis and precipitation thereof. It was also observed that the dimerisation reaction process steps to stabilise the ions in solution also evolved H^+ ions, which maintained the pH within the specified ranges. This has the advantage that it is not necessary to top-up the acid during the acid leaching process step.

However, it must be noted that this observation is attributed to the low concentration of acid-consuming impurities, specifically excess Li. Hence, considering that thus far in the CSIR system the excess Li concentration is subject to experimental uncertainty as it varies per campaign depending on the location of the crude sample in the lithiothermic reactor vessel, the consumption of the HCl can be higher, even though this could not be proven in this test work. The pH observations showed that initial acid concentrations of 1 M and 0.032 M are efficient to circumvent the formation of hydrolysis products, as recommended by Seon and Nataf (1988).

Characterisation of the leached residue by SEM showed proof of sintering and mechanical occlusion by jaw crushing. This indicates that an increase in residence time, in addition to

temperature, will not lead to additional extraction of LiCl. Consequently, for any hypothesis based on the effect of time or increase in residence time to be true, the titanium powder or sponge pores must not be closed by either sintering, crushing or by a combination of both. The kinetics of the dissolution followed a shrinking-core model with HER on the surface of the particle as the rate-controlling step. A phenomenon assumed to be attributed to some excess by-products that were not dissolved completely during acid and due to the increased residence time during water washing were dissolved to evolve hydrogen gas .

The information obtained in this study can be used by CSIR as a baseline for developing a process flow sheet, selecting leaching process parameter ranges and for modelling purposes. The data regarding the temperature may be used to design the cooling system, size the leaching vessel and its components.

Although not investigated in this study, it would be interesting to identify and characterise the oxygen impurities to elucidate whether the oxygen impurities exist as interstitial impurities or surface oxide layer. It is recommended that the chloride impurities in the product be characterised to confirm whether they are present as residual LiCl or oxychlorides. Furthermore, it is recommended that the by-products dissolution mechanism be investigated. The leached residues should be subjected to moisture analysis to determine the amount of water that can absorbed by occluded LiCl. This will assist in establishing the extent of the effect of hygroscopicity of LiCl on the residual impurities, storage and requirements downstream.

6 REFERENCES

Aleksandrovskii, S. V., Berdnikova, L. M., Lukashenko, G. S., Pinaev, E. N., & Snisar, G. P. (1982). Conversion of a sodium-thermic reaction mass into titanium powders. *Soviet Powder Metallurgy and Metal Ceramics, 21*(1), 4–7. https:// doi.org/10.10

Ashton, J. F. (1977). *Some Aspects of the Solution Chemistry of Titanium (III)* [Masters Thesis, University of Tasmania]. https:// eprints.utas.edu.au/19394/1/whole_AshtonJohnFrederick1977_thesis.pdf.

Baril, E., Lefebvre, L. P., & Thomas, Y. (2011). Interstitial elements in titanium powder metallurgy: Sources and control. *Powder Metallurgy, 54*(3), 183–186. https:// doi.org/10.1179/174329011X13045076771759

Bolivar, R., & Friedrich, B. (2019). Magnesiothermic reduction from titanium dioxide to produce titanium powder. *Journal of Sustainable Metallurgy, 5*(2), 219–229. https:// doi.org/10.1007/s40831-019-00215-z

Boozenny, A., Kleinman, M. H., & Tarsey, A. R. (1961). *Purification of crude titanium metal* (U.S. Patent No. 2992098). U. S. Patent and Trademark Office.

Cassaignon, S., Koelsch, M., & Jolivet, J. P. (2007). From $TiCl_3$ to TiO_2 nanoparticles (anatase, brookite and rutile): Thermohydrolysis and oxidation in aqueous medium. *Journal of Physics and Chemistry of Solids, 68*(5-6), 695–700. https:// doi.org/10.1016/j.jpcs.2007.02.020

Choi, S. H., Sim, J. J., Lim, J. H., Seo, S. J., Kim, D. W., Hyun, S. K., & Park, K. T. (2019). Removal of Mg and MgO by-products through magnesiothermic reduction of Ti powder in self-propagating high-temperature synthesis. *Metals, 9*(2), 169. https:// doi.org/10.3390/met9020169

Chown, L. (2016). Quo vadis titanium?. *Mechanical Technology*, 26.

Clark, R. J. H. (1973). The Chemistry of Titanium. In J. C. BailerJr., H. J. Emeleus., R. Nyholm. & A. F. Trotman-Dickenson (Eds.), *Comprehensive Inorganic Chemistry* (pp. 355–417). Oxford, United Kingdom: Pergamon Press.

Cotton, F. A., & Wilkinson, G. (1980). *Advanced Inorganic Chemistry: A Comprehensive Text* (4th ed.). New York, NY: John Wiley & Sons.

Crowli, G. (2003). How to extract low-cost titanium. *Advanced Materials and Processes, 161*(11), 25–27.

Cservenyak, I., Kelsall, G. H., & Wang, W. (1996). Reduction of tilV species in aqueous sulfuric and hydrochloric acids i. titanium speciation. *Electrochimica Acta, 41*(4), 563–572. https:// doi.org/10.1016/0013-4686(95)00343-6

Fang, Z. Z., Paramore, J. D., Sun, P., Chandran, K. S. R., Zhang, Y., Xia, Y., Cao, F., Koopman, M., & Free, M. (2018). Powder metallurgy of titanium–past, present, and future. *International Materials Reviews*, *63*(7), 407–459. https:// doi.org/10.1080/09506608.2017.1366003

Free, M. L. (2013). *Hydrometallurgy: Fundamentals and Applications*. Hoboken, NJ: John Wiley & Sons.

Froes, F. H., & Imam, M. A. (2010). Cost affordable developments in titanium technology and applications. *Key Engineering Materials, 436*, 1–11. https:// doi.org/10.4028/www.scientific.net/kem.436.1

Gale, W. F., & Totemeier, T. C. (2004). *Smithells Metals Reference Book* (8th ed.). Oxford, United Kingdom: Elsevier.

Gambogi, J., & Gerdemann, S. J. (1999). Titanium metal: extraction to application. Review of extraction, processing, properties & applications of reactive metals. In B. Mishra (Ed.), *The Minerals, Metals & Materials Society Annual Meeting* (pp. 175–210). San Diego, CA: Wiley.

Gardner, H. J. (1967). Chloroaquo complexes of titanium(III): The 2T2g→2Eg absorption band. *Australian Journal of Chemistry, 20*(11), 2357–2365. https:// doi.org/10.1071/ch9672357

Garmata, V. A., Gulyanitskii, B. S., Lipkes, Y. M., Seryakov, G. V., & Kramnik, V. Y. (1970). *The metallurgy of titanium*. In National Technical Information Service (1st ed.). Springfield, IL: Wright Patterson Air Force Base OH.

Goso, X., & Kale, A. (2011). Production of titanium metal powder by the HDH process. *Journal of The Southern African Institute of Mining and Metallurgy, 111*(3), 203–204.

Gould, E. S. (2011). Redox chemistry of aquatitanium(II), Ti^{2+}(aq). *Coordination Chemistry Reviews, 255*(23–24), 2882–2891. https:// doi.org/10.1016/j.ccr.2011.06.006

Habashi, F. (1997). *Handbook of Extractive Metallurgy*. New York, NY: Wiley-VCH.

Habashi, F. (1999). *Textbook of Hydrometallurgy* (2nd ed.). Quebec, Canada: Métallurgie Extractive Québec.

Hansen, D. A., & Gerdemann, S. J. (1998). Producing titanium powder by continuous vapor-phase reduction. *JOM, 50*(11), 56–58. https:// doi.org/10.1007/s11837-998-0289-3

Ivanov, S. L., & Zablotsky, D. (2018). A feasibility study for high-temperature titanium reduction from $TiCl_4$ using a magnesiothermic process. *IOP Conference Series: Materials Science and Engineering 355*(1), 012010. https:// doi.org/10.1088/1757-899x/355/1/012010

Jamrack, W. D. (1963). *Rare Metal Extraction by Chemical Engineering Techniques*. Oxford, United Kingdom: Pergamon.

Jeppson, D. W., Ballif, J. L., Yuan, W. W., & Chou, B. E. (1978). *Lithium literature review : Lithium's properties and interactions (Report No. HEDL-TME-78-15)*. Richland, DC: Hanford Engineering Development Laboratory.

Kelly, E. J. (1982). Electrochemical Behaviour of Titanium. In J. Bockris, B. Conway & R. White (Eds.), *Modern Aspects of Electrochemistry: No. 14*, (pp. 319–417). New York, NY: Plenum Press. https:// doi.org/10.1136/bmj.1.3567.930-a

Kelly, J. T. (1963). *Metal purification process* (U.S. Patent No. 3085874). U.S Patent and Trademark Office.

Kohli. (1981). *The production of titanium from ilmenite: A review (Report No. LBL-13705UC-25)*. Lawrance Berkley Laboratory: University of California Materials & Molecular Research Division.

Kölle, U., & Kölle, P. (2003). Aqueous chemistry of titanium(II) species. *Angewandte Chemie International Edition, 42*(37), 4540–4542. https:// doi.org/10.1002/anie.200351280

Liang, L., Dachun, L., Heli, W., Kaihua, L., Juhai, D., & Wenlong, J. (2018). Removal of chloride impurities from titanium sponge by vacuum distillation. *Vacuum,* 152, 166–172. https:// doi.org/10.1016/j.vacuum.2018.02.030

Liang, L., Fuxing, Z., Dachun, L., Kaihua, L., Zhuo, S., & Baoqiang, X. (2019). Influence factors analysis on scavenging of chlorine impurity from crude titanium sponge. In Jiang, T., Hwang, J., Gregurek, D., Peng, Z., Downey, J. P., Zhao, O. Y., Keskinkilic, E., & Padilla, R. (Eds.), *10th International Symposium on High-Temperature Metallurgical Processing* (pp. 681–691). Springer. https:// doi.org/10.1007/978-3-030-05955-2

Liang, L., Zhu, F., Deng, P., Jia, Y., Kong, L., Deng, B., Li, K., & Liu, D. (2020). Separation and recycling of chloride salts from electrolytic titanium powders by vacuum distillation. *Separation and Purification Technology,* 236, 116282. https:// doi.org/10.1016/j.seppur.2019.116282

Low, R. J., Qian, M., & Schaffer, G. B. (2012). Chloride impurities in titanium powder metallurgy—A review. *Proceedings of the 12th World Conference on Titanium,* 3, 1770–1774. Beijing, China: Science Press Beijing.

Mackenzie, H. A. E., & Tompkins, F. C. (1942). The kinetics of the autoxidation of inorganic reducing agents. Part I.—Titanous chloride. *Transactions of the Faraday Society, 38*, 465-473. https:// doi.org/10.1039/tf9423800465

McKinley, T. D. (1955). *Recovery of titanium metal* (U.S. Patent No. 2707149). U.S. Patent and Trademark Office.

Menzies, I. A., & Averill, A. F. (1968). The anodic behaviour of titanium in HCl-methanol solutions. *Electrochimica Acta, 13*(4), 807–824. https:// doi.org/10.1016/0013-4686(68)85013-3

Monnin, C., Dubois, M., Papaiconomou, N., & Simonin, J. P. (2002). Thermodynamics of the LiCl + H_2O system. *Journal of Chemical & Engineering Data, 47*(6), 1331–1336.

Montgomery, D. C. (2017). *Design and Analysis of Experiments* (9th ed.). Hoboken, NJ: Wiley.

Nabivanets, B. I. (1965). The use of ion-exchange chromatography for studying the state of ions of high-valency elements in solution. *Russian Chemical Reviews, 34*(5), 392–402. https:// doi.org/10.1070/rc1965v034n05abeh001452

Nagesh, C. R. V. S., Ramachandran, C. S., & Subramanyam, R. B. (2008). Methods of titanium sponge production. *Transactions of the Indian institute of Metals, 61*(5), 341–348. https:// doi.org/10.1007/s12666-008-0065-7

Nagesh, C. R. V. S., Rao, C. S., Ballal, N. B., & Rao, P. K. (2004). Mechanism of titanium sponge formation in the kroll reduction reactor. *Metallurgical and Materials Transactions B, 35*(1), 65-74. https// doi.org/10.1007/s11663-004-0097-2

Nagesh, C.R. V. S., Sitarama, T. S., Ramachandran, C. S., & Subramanyam, R. B. (1994). Development of indigenous technology for production of titanium sponge by the Kroll process. *Bulletin of Materials Science, 17*(6), 1167–1179. https:// doi.org/10.1007/bf02757594

Nechaev, N. P., & Polezhaev, E. V. (2016). Effect of physicochemical treatment on titanium porous powder quality. *Metallurgist, 60*(3–4), 339–341. https:// doi.org/10.1007/s11015-016-0296-5

Nicholls, D. (2017). *Complexes and First-Row Transition Elements*. London, England: Macmillian.

Okabe, T. H., & Waseda, Y. (1997). Producing titanium through an electronically mediated reaction. *JOM, 49*(6), 28-32. https:// doi.org/10.1007/bf02914710

Oosthuizen, S. J. (2011). Titanium: the innovators' metal—Historical case studies tracing titanium process and product innovation. *Journal of the Southern African Institute of Mining and Metallurgy, 111*(11), 781–786.

Oosthuizen, S. J., & Swanepoel, J. J. (2018). Development status of the CSIR-Ti process. *IOP Conference Series: Materials Science and Engineering,* 430, 012008. https:// doi.org/10.1088/1757-899x/430/1/012008

Park, S. H., Batchelor, B., Lee, C., Han, D. S., & Abdel-Wahab, A. (2012). Perchlorate degradation using aqueous titanium ions produced by oxidative dissolution of zero-valent titanium. *Chemical Engineering Journal, 192*, 301–307. https:// doi.org/10.1016/j.cej.2012.04.013

Pecsok, R. L., & Fletcher, A. N. (1962). Hydrolysis of titanium (III). *Inorganic Chemistry, 1*(1), 155–159. https:// doi.org/10.1021/ic50001a031

Peter, W. H., Chen, W., Yamamoto, Y., Dehoff, R., Muth, T., Nunn, S. D., Kiggans, J. O., Clark, M. B., Sabau, A .S., Gorti, S., Blue, C. A., & Williams, J. C. (2012). Current status of Ti-PM: Progress, opportunities and challenges. *Key Engineering Materials, 520*, 1–7. https:// doi.org/10.4028/www.scientific.net/kem.520.1

Poulsen, E. R., & Hall, J. A. (1983). Extractive metallurgy of titanium: A review of the state of the art and evolving production techniques. *JOM, 35*(6), 60–65. https:// doi.org/10.1007/BF03338304

Pourbaix, M. J. N. (1974). *Atlas of Electrochemical Equilibria in Aqueous Solutions: Translated from the French except sections I, III 5, III 6 which were originally written in English* (J. Franklin, Trans.). Houstin, Tex: National Association of Corrosion Engineers.

Qian, M., Schaffer, G. B., & Bettles, C. J. (2010). Sintering of titanium and its alloys. In Z. Z. Fang (Eds.), *Sintering of Advanced Materials: Fundamentals and processes* (pp. 324–355). Oxford, United Kingdom: Woodhead Publishing. https:// doi.org/10.1533/9781845699949.3.324

Richardson, J. F., Harker, J.H., Backhurst, J. R., &. Coulson, J. M. (2002). *Coulson and Richardson's Chemical Engineering: Vol 2*. Oxford, United Kingdom: Butterworth-Heinemann

Richens, D. T. (1997). *The Chemistry of Aqua Ions*. Chichester, England: Wiley.

Sarswat, P. K. (2010). *A study of Integrated Leaching and Electrowinning of Copper from Chalcopyrite Ore Using Chloride Media* [Masters dissertation, Department of Metallurgical Engineering, University of Utah]. https:// collections.lib.utah.edu/ark:/87278/s6pc3gw3

Sekimoto, H., Nose, Y., Uda, T., & Sugimura, H. (2010). Quantitative analysis of titanium ions in the equilibrium with metallic titanium in NaCl-KCl equimolar molten salt. *Materials Transactions, 51*(11), 2121–2124. https:// doi.org/10.2320/matertrans.M2010238

Seon, F., & Nataf, P. (1988). *Production of metals by metallothermia* (U.S. Patent No. 4725312). U.S. Patent and Trademark Office.

Shuvalov, V. F., Solov'ev, S. L., & Lebedev, Y. S. (1978). ESR investigation of the hydrolysis of titanium(III) in aqueous hydrochloric acid solutions. *Bulletin of the Academy of Sciences of the USSR Division of Chemical Science, 27*(1), 5–9.

https:// doi.org/10.1007/bf01153196

Sole, K. C. (1999). Recovery of titanium from the leach liquors of titaniferous magnetites by solvent extraction: Part 1. Review of the literature and aqueous thermodynamics. *Hydrometallurgy, 51*(2), 239–253. https:// doi.org/10.1016/s0304-386x(98)00081-4

Straumanis, M. E., & Chen, P. C. (1951). The corrosion of titanium in acids—The rate of dissolution in sulfuric, hydrochloric, hydrobromic and hydroiodic acids. *Corrosion, 7*(7), 229–237. https://doi.org/10.5006/0010-9312-7.7.229

Sun, P., Fang, Z. Z., Zhang, Y., & Xia, Y. (2017). Review of the methods for production of spherical Ti and Ti Alloy powder. *JOM, 69*(10), 1853–1860. https:// doi.org/10.1007/s11837-017-2513-5

U. S. Geological Survey. (2020). *Mineral Commodity Summaries 2020.* https://doi.org/10.3133/mcs2020.ISBN

Van Tonder, W. (2010). *South African Titanium: Techno-Economic Evaluation of the Alternatives to the Kroll Process* [Masters dissertation, Stellenbosch University]. http:// hdl.handle.net/10019.1/4142

Van Vuuren, D. S. (2009). A critical evaluation of processes to produce primary titanium. *Journal of the Southern African Institute of Mining and Metallurgy, 109*, 455–461.

Van Vuuren, D. S., & Oosthuizen, S. J. (2014). *Titanium powder production process* (U. S. Patent No. 8790441). U.S. Patent and Trademark Office.

Van Vuuren, D. S., Oosthuizen, S. J., & Heydenrych, M. D. (2011). Titanium production via metallothermic reduction of $TiCl_4$ in molten salt: Problems and products. *Journal of the Southern African Institute of Mining and Metallurgy, 111*(3), 141–147.

Wang, Q., Song, J., Hu, G., Zhu, X., Hou, J., Jiao, S., & Zhu, H. (2013). The equilibrium between titanium ions and titanium metal in NaCl-KCl equimolar molten salt. *Metallurgical and Materials Transactions B, 44*(4), 906–913. https:// doi.org/10.1007/s11663-013-9853-5

Wasz, M. L., Brotzen, F. R., McLellan, R. B., & Griffin, A. J. (1996). Effect of oxygen and hydrogen on mechanical properties of commercial purity titanium. *International Materials Reviews, 41*(1), 1–12. https:// doi.org/10.1179/imr.1996.41.1.1

Withers, J. C., Shapovalov, V., Storm, R., & Loutfy, R. O. (2013). The production of titanium alloy powder. *Key Engineering Materials*, 551, 32–36. https:// doi.org/10.4028/www.scientific.net/KEM.551.32

Xia, Y., Zhao, J., Tian, Q., & Guo, X. (2019). Review of the effect of oxygen on titanium and deoxygenation technologies for recycling of titanium metal. *JOM, 71*(9), 3209–3220. https:// doi.org/10.1007/s11837-019-03649-8

Yakovleva, E. G., Pechurova, N. I., Martynenko, L. I., & Spitsyn, V. I. (1973). Study of the complex formation of Ti(III) with nitrilotriacetic and diethylenetriaminepentaacetic acids in aqueous solution. *Bulletin of the Academy of Sciences of the USSR Division of Chemical Science, 22*(8), 1655-1657.https:// doi.org/10.1007/bf00932086

Yan, M., Tang, H. P., & Qian, M. (2015). Scavenging of oxygen and chlorine from powder metallurgy (PM) titanium and titanium alloys. In M. A. Qian & F. H. Froes (Eds.), *Titanium Powder Metallurgy* (pp. 253–276). Oxford, United Kingdom: Butterworth-Heinemann. https:// doi.org/10.1016/B978-0-12-800054-0.00015-0

Yang, X. (2019). *Leaching Characteristics of Rare Earth Elements from Bituminous Coal-Based Sources*. (Doctoral dissertation, University of Kentucky). https:// uknowledge.uky.edu/mng_etds/49

Yang, Z., & Gould, E. S. (2005). Reductions by aquatitanium(II). *Dalton Transactions,* 10, 1781–1784. https:// doi.org/10.1039/b416975c

Yu, C. Z., & Jones, M. I. (2013). Investigation of chloride impurities in hydrogenated–dehydrogenated Kroll processed titanium powders. *Powder Metallurgy, 56*(4), 304–309. https:// doi.org/10.1179/1743290113y.0000000055

Zhu, Z., Zhang, W., & Cheng, C. Y. (2011). A literature review of titanium solvent extraction in chloride media. *Hydrometallurgy, 105*(3–4), 304–313. https:// doi.org/10.1016/j.hydromet.2010.11.006

7 APPENDICES

Appendix 1: Summary of the leaching conditions

Test No	Initial concentration (M)	Initial temperature (°C)	Stirring rate (rpm)	Particle size (mm)	Solid/liquid (g/ml)	Initial oxygen (m%)	Initial chloride (m%)
1	0.032	14	400	−10	20/200	0.02	0.30
2	1	14	400	−10	20/200	0.02	0.30
3	0.032	14	400	+10	20/200	0.02	0.30
4	1	14	400	+10	20/200	0.02	0.30
5	0.032	30	400	−10	20/200	0.02	0.30
6	1	30	400	−10	20/200	0.02	0.30
7	0.032	30	400	+10	20/200	0.02	0.30
8	1	30	400	+10	20/200	0.02	0.30

Appendix 2: Factorial design equations

$$(A) = (-Y_1 + Y_2 - Y_3 + Y_4 - Y_5 + Y_6 - Y_7 + Y_8)/8 \quad 7.1$$

$$(B) = (-Y_1 - Y_2 + Y_3 + Y_4 - Y_5 - Y_6 + Y_7 + Y_8)/8 \quad 7.2$$

$$(B) = (-Y_1 - Y_2 + Y_3 + Y_4 - Y_5 - Y_6 + Y_7 + Y_8)/8 \quad 7.3$$

$$(AB) = (Y_1 - Y_2 - Y_3 + Y_4 + Y_5 - Y_6 - Y_7 + Y_8)/8 \quad 7.4$$

$$(BC) = (Y_1 + Y_2 - Y_3 - Y_4 - Y_5 - Y_6 + Y_7 + Y_8)/8 \quad 7.5$$

$$(AC) = (Y_1 - Y_2 + Y_3 - Y_4 - Y_5 + Y_6 - Y_7 + Y_8)/8 \quad 7.6$$

$$(ABC) = (-Y_1 + Y_2 + Y_3 - Y_4 + Y_5 - Y_6 - Y_7 + Y_8)/8 \quad 7.7$$

Appendix 3: Test No 1–8 temperature and pH raw data

Appendix 3.1: Temperature readings for all the acid leaching experiments

	Sample ID							
Time (min)	Test No 1	Test No 2	Test No 3	Test No 4	Test No 5	Test No 6	Test No 7	Test No 8
0	14	14	14	14	30	30	30	30
5	30	29	27	28.8	55	58	52.6	54
10	26.8	26	25	25.9	51	52	49	50
15	25.7	24.7	23.8	22.3	45	47	45	43
30	21.3	21	25.2	25.2	38	39.4	36	37.2
60	22.5	20.9	25	26.2	33.9	34.3	34.8	35.6

Appendix 3.2: pH readings for all the acid leaching experiments

	Sample ID							
Time (min)	Test No 1	Test No 2	Test No 3	Test No 4	Test No 5	Test No 6	Test No 7	Test No 8
0	1.5	0	1.48	0	1.52	0	1.54	0
5	1.61	0.43	1.59	0.47	1.65	0.42	1.62	0.53
10	1.27	0.24	1.36	0.29	1.21	0.17	1.31	0.2
15	1.25	0.23	1.24	0.27	1.19	0.16	1.23	0.22
30	1.25	0.25	1.21	0.19	1.17	0.19	1.26	0.35
60	1.23	0.22	1.28	0.19	1.18	0.16	1.26	0.14

Appendix 4: Leaching experiments raw data for the kinetic modelling studies

The pH, temperature measurements as well as conductivity measurements during washing. Cumulative time for each cycle was established by combining the time at each interval i.e., cycle 1 = 0 + 120 which is 120, Cycle 2 = 120+ cycle 1 = 0 min + 120 min which is 120, Cycle 2 = 120 min + 180 min which is 300 min; cycle 3 = 420 min and cycle 4 = 480 min.

Test No 1: **−10 mm**

Acid leaching at 14°C		
Time (min)	pH	T(°C)
0	1.50	16.3
5	1.55	30.0
10	1.37	26.8
15	1.25	25.7
30	1.25	25.2
60	1.23	25.0

De-ionised water washing at 14°C		
Time (min)	Cycle No	Conductivity µm
0	Fresh water	14
120	1	2999 (above limit)
180	2	113
120	3	37
60	4	16

Test No 3: **+10 mm**

Acid leaching at 14°C		
Time (min)	pH	T(°C)
0	1.48	15.2
5	1.54	29.0
10	1.36	27.1
15	1.24	26.0
30	1.21	25.9
60	1.21	25.7

De-ionised water washing at 14°C		
Time (min)	Cycle No	Conductivity µm
0	Fresh water	14
120	1	2999 (above limit)
180	2	119
120	3	41
60	4	18

Test No 5: **−10 mm**

Acid leaching at 30°C		
Time (min)	pH	T(°C)
0	1.52	32.4
5	1.60	55.1
10	1.25	49.1
15	1.19	45.2
30	1.17	37.5
60	1.18	35.0

De-ionised water washing at 30°C		
Time (min)	Cycle No	Conductivity µm
0	Fresh water	14
120	1	2999 (above limit)
180	2	167
120	3	52
60	4	18

Test No 7: **+10 mm**

Acid leaching at 30°C		
Time (min)	pH	T(°C)
0	1.54	34.2
5	1.65	58.5
10	1.31	51.2
15	1.23	47.2
30	1.26	44.3
60	1.26	35.7

De-ionised water washing at 30°C		
Time (min)	Cycle No	Conductivity µm
0	Fresh water	14
120	1	2999 (above limit)
180	2	145
120	3	34
60	4	15

Appendix 5: Percentage cumulative chloride removal calculations and kinetic modelling calculations for the different rate–controlling steps

Appendix 5.1: Cumulative % chloride removal

Time	Leaching Test No			
	Test No 1	Test No 3	Test No 5	Test No 7
0	0.00	0.00	0.00	0.00
120	0.13	0.10	0.23	0.10
300	0.37	0.17	0.53	0.27
420	0.50	0.23	0.77	0.47
480	0.57	0.27	0.87	0.53

Appendix 5.2: Reaction control mechanism calculations

Time	$K_r t = 1 - (1 - x)^{1/3}$			
	Test No 1	Test No 3	Test No 5	Test No 7
0	0.000	0.000	0.000	0.000
120	0.047	0.035	0.085	0.035
300	0.141	0.059	0.224	0.098
420	0.206	0.085	0.385	0.189
480	0.243	0.098	0.490	0.224

Appendix 5.3: Diffusion control mechanism calculations

Time	$K_d t = 1 + 2(1 - x) - 3(1 - x)^{2/3}$			
	Test No 1	Test No 3	Test No 5	Test No 7
0	0.000	0.000	0.000	0.000
120	0.006	0.003	0.020	0.003
300	0.054	0.010	0.128	0.027
420	0.110	0.020	0.330	0.094
480	0.149	0.027	0.484	0.128

Appendix 6: Experimental repeatability test

To evaluate repeatability, Test Nos 3 and 8 were repeated. The oxygen and chloride analysis results, raw data for both pH and temperature displayed on Appendix 6.1– 6.3. The oxygen and chloride analysis in the purified product was used to calculate standard deviation and error as shown in Appendix 6.4.

Appendix 6.1: Design matrix of the 2^3 level full factorial design, inclusive of the repeats

				Assay Results	
Test No	*A* (M)	*B* (mm)	*C* (°C)	Response 1 (oxygen m%)	Response 2 (chloride m%)
3(a)	0.032 (−1)	+10 (+1)	14 (−1)	0.07	0.22
3(b)	0.032 (−1)	+10 (+1)	14 (−1)	0.11	0.25
8(a)	1.0 (+1)	+10 (+1)	30 (+1)	0.41	0.10
8(b)	1.0 (+1)	+10 (+1)	30 (+1)	0.40	0.10

Appendix 6.2: Temperature readings inclusive of the repeats

	Sample ID			
Time (min)	Test No 3(a)	Test No 3(b)	Test No 8(a)	Test No 8(b)
0	14	13.8	30	30.2
5	27	26.6	54	53.5
10	25	23.4	50	54.2
15	23.8	19.8	43	47.2
30	25.2	19.1	37.2	40.3
60	25	18.6	35.6	38.0

Appendix 6.3: pH readings inclusive of the repeats

	Sample ID			
Time (min)	Test No 3(a)	Test No 3(b)	Test No 8(a)	Test No 8(b)
0	1.48	1.5	0	0
5	1.59	1.57	0.53	0.55
10	1.36	1.40	0.20	0.28
15	1.24	1.34	0.22	0.23
30	1.21	1.24	0.35	0.35
60	1.28	1.28	0.14	0.16

Appendix 6.4: Statistical analysis of the oxygen and chloride assays

Sample ID	Average $(\bar{x}) = \frac{\sum_i^n x_i}{n}$	Standard deviation $(s) = \sqrt{\frac{[\sum_1^n x_i^2]-n\bar{x}^2}{n-1}}$	Standard error $s_{\bar{x}} = \frac{s}{\sqrt{n}}$
Test No 3 (oxygen)	0.090	0.028	0.020
Test No 3 (chloride)	0.235	0.021	0.015
Test No 8 (oxygen)	0.405	0.007	0.000
Test No 8 (chloride)	0.100	0.005	0.000

Where *n* = sample size and $s_{\bar{x}}$ = standard error, which is used in place of the standard deviation when comparing data set (Free, 2013; Montgomery, 2017).

Appendix 6.4 showed a variance between the results, as both the standard deviation and standard error for oxygen and chloride content in both Test Nos 3 and 8 was > 0, except for Test No 8 chloride content, which was equal to zero. However, all the variances were close to zero. Thus, it may be concluded that the procedure is precise and reproducible.